ORIGINAL ARTICLE

A new robust modified capuchin search algorithm for the optimum amalgamation of DSTATCOM in power distribution networks

Mohamed A. Tolba[1] · Essam H. Houssein[2] · Mohammed Hamouda Ali[3] · Fatma A. Hashim[4,5]

Abstract

Very sensitive loads require the safe operation of electrical distribution networks, including hospitals, nuclear and radiation installations, industries used by divers, etc. To address this issue, the provided paper suggests an innovative method for evaluating the appropriate allocation of Distribution STATic COMpensator (DSTATCOM) to alleviate total power losses, relieve voltage deviation, and lessen capital annual price in power distribution grids (PDGs). An innovative approach, known as the modified capuchin search algorithm (mCapSA), has been introduced for the first time, which is capable of addressing several issues regarding optimal DSTATCOM allocation. Furthermore, the analytic hierarchy process method approach is suggested to generate the most suitable weighting factors for the objective function. In order to verify the feasibility of the proposed mCapSA methodology and the performance of DSTATCOM, it has been tested on two standard buses, the 33-bus PDG and the 118-bus PDG, with a load modeling case study based on real measurements and analysis of the middle Egyptian power distribution grid. The proposed mCapSA technique's accuracy is evaluated by comparing it to other 7 recent optimization algorithms including the original CapSA. Furthermore, the Wilcoxon sign rank test is used to assess the significance of the results. Based on the simulation results, it has been demonstrated that optimal DSTATCOM allocation contributes greatly to the reduction of power loss, augmentation of the voltage profile, and reduction of total annual costs. As a result of optimized DSTATCOM allocation in PDGs, distribution-level uncertainties can also be reduced.

List of symbols

$Q_{\text{DSTATCOM},i}$	Reactive power injected by DSTATCOM
MObjF	Multi-objective function
$V_{\text{new},i}$	Absolute voltage at node i
κ_1, κ_2, κ_3, and κ_4	Weighting factors of the objective function
$P_{\text{Loss}(i,j)}$, $Q_{\text{Loss}(i,j)}$	Active and reactive power losses, respectively through "i-bus" and "j-bus"
$P_{\text{TLoss},b}$	Total base power losses

✉ Mohamed A. Tolba
  matolba@eaea.org.eg

Essam H. Houssein
  essam.halim@mu.edu.eg

Mohammed Hamouda Ali
  Eng_MohammedHamouda@azhar.edu.eg

Fatma A. Hashim
  fatma_hashim@h-eng.helwan.edu.eg

1   Reactors Department, Nuclear Research Center, Egyptian Atomic Energy Authority (EAEA), Cairo 11787, Egypt

2   Faculty of Computers and Information, Minia University, Minia 61519, Egypt

3   Department of Electrical Engineering, AL-Azhar University, Cairo, Egypt

4   Faculty of Engineering, Helwan University, Cairo 11795, Egypt

5   MEU Research Unit, Middle East University, Amman 11831, Jordan

$P_{\text{DST,TLoss}}$	System active losses including DSTATCOMs
IVD_b	Index of the voltage deviation at the basic-scenario
IVD_{DST}	Index of the voltage deviation with DSTATCOM location
V_{max}, V_{min}	Maximum and minimum voltage levels, respectively
$V_{i,\text{DST}}$, $V_{i,b}$	Voltage with DSTATCOM and the base one, respectively
IVSD_b	Index of the voltage stability deviation at the base case
IVSD_{DST}	Index of the voltage stability deviation with DSTATCOM
VS, VS_{max}	Voltage stability and its maximum value, respectively
En_b, En_{DST}	Energy price before and after allocating the DSTATCOM, respectively
C_{en}	Coefficient of the energy price rate (60 \$/MWh)
β_{DST}	Operational cost of the Q_{DSTATCOM}
β_{Loc}	Investment price of the Q_{DSTATCOM} location
Ψ_{DST}	Reactive power set 0 or 1
I_{CI} and I_{RI}	Consistency and random indexes, respectively
$P_{j,\text{eff}}$ and $Q_{j,\text{eff}}$	Effective values of active and reactive loads
λ_{max}	Maximum eigenvalue

1 Introduction

A typical power distribution grid (PDG) has a radial structure since it is easier to protect and has a reduced short circuit level. A distribution system delivers power to clients to meet their needs. It has the highest losses as compared to the generating and transmission systems due to low voltage, high current flow, a high R/X ratio, and the radial nature [1, 2]. According to the literature, about 10–13% of total generated power is squandered as I^2R losses in PDG [3]. Researchers have paid close attention to distribution networks in recent years because they play an imperative role in the quality and planning of power systems. Power quality degradation impacts a number of significant demands. These may include divers' heavy industries, hospitals, emergency systems, and nuclear and radiation installations. For example according to the international atomic authority section [2, 4], the research reactors are

suffering from interruptions in voltage profiles that may cause Loss of Off-site Power Supply (LOPS). A reliable on-site power supply with reliable power quality is crucial for ensuring the safety of nuclear reactors as well as safeguarding the public and the environment from the radioactive dangers posed by LOPS. By installing appropriate compensatory devices, distribution system losses can be minimized. In this regard, capacitors are critical in decreasing power losses in PDG. It is also possible to increase voltage levels across buses using capacitors; however, providing a variable reactive power source is extremely challenging [5, 6]. As a result, distributors must account for these capacitor costs as well as installing them in appropriate places with optimal sizes. Another problem with capacitor placement is that load balancing is not possible due to capacitor operating issues such as resonance. Furthermore, one of the key complications associated with the use of capacitors in PDG is the oscillation in nature of capacitor devices when compared to inductive components with comparable circuits [7]. To address these issues, Distributed Flexible Alternating Current Transmission Systems (D-FACTS) are utilized in PDGs to minify power losses and increase bus voltages. D-FACTS devices can offer higher performance and lower-cost way of improving network controllability and reliability, increasing asset utilization, and improving end-user power quality while minimizing environmental impact and system cost [8–11]. Presently, quality issues in electrical power networks are becoming more sophisticated at all levels. As a result, maintaining appropriate levels of electric power quality is a considerable task [10].

Distribution Static Compensator (DSTATCOM) and Static Var Compensator (SVC) are the most commonly utilized D-FACTS devices. As evidenced in previous studies [12–17], the DSTATCOM is the preferred appropriate device since it provides excellent reactive power while preventing unbalanced loading in PDG. Furthermore, it has outstanding characteristics such as no resonance or transient harmonics troubles, low harmonic content output, and small footprint [12, 13]. Voltage source converters are used in customized DSTATCOM devices. It can also function as a shunted device, capacitor connection, and conjunction transformer. It is used to regulate system bus voltages, control power factor, real power, and reactive power. DSTATCOM can supply capacitive and inductive modal adjustment that is both quick and permanent [14]. DSTATCOM is the most effective device for eliminating harmonic deformity from the system and avoiding imbalance [15]. DSTATCOM deployment maximizes annual cost savings, lowers power losses, increases load ability, boosts stability, adapts for reactive power, and maintains power quality [16]. Ultimately, DSTATCOM has numerous benefits, including low power losses, low harmonic

output, robust regulatory capabilities, relatively inexpensive, and tiny size [17]. Consequently, finding the most effective allocation of DSTATCOM has a serious influence on PDG. Table 1 outlines the primary advantages and purposes of DSTATCOM and SVC.

1.1 Literature review

DSTATCOM allocations have received little attention from researchers. So far, different strategies for DSTATCOM allocation have been adopted, including (1) modal analysis, (2) analytical techniques, and (3) optimization algorithms.

Originally, modal analysis approaches and time-domain simulation were employed to solve the DSTATCOM determination issue in the distribution systems (DS) to foster power goodness [18].

Analytical approaches, on the other hand, are employed to tackle DSTATCOM layout issues in PDG for loss relief and bus voltage augmentation [19]. The power loss index (PLI) is taken into account while resolving DSTATCOM allocation concerns in PDG [20]. The voltage stability index (VSI) has been determined before locating the DSTATCOM devices optimally in different PDGs [21]. The PLI and VSI are taken into account while resolving DSTATCOM allocation concerns in PDGs [22, 23]. In [24], the VSI has been employed to elect the candidate nodes for locating the DSTATCOM devices. For handling uncertain attributes of loads by [25], the Monte Carlo simulation (MCS) technique is applied. The analytical approach-based technique has been utilized to deduce the allocation of distributed generators (DG) and DSTATCOM based on the VSI and loss sensibility factor (LSF) [26].

Numerous researches have focused on recent techniques and methodologies. However, these researches can be divided in two categories.

In the first category, many researchers considered the study of the optimum allocation of DSTATCOM. Like the

particle swarm optimization (PSO) [27], bacterial foraging optimization algorithm (BFOA) [28], and echolocation-based bat algorithm (EBA) [29] have been introduced to minify the losses and operational costs, as well as to enhance the voltage profile in PDG. The multi-objective genetic algorithm (MOGA) [30] has been developed to consider the average current total harmonic distortion (THD) and the overall operational prices as the main objective function (ObjF). Differential evolution (DE) and long-term planning of DSTATCOM allocation have been proposed to maximize the total net profit (TNP) with annual savings price and minimize the energy price [31]. Based on the modified crow search algorithm (MCSA) developed [32], with the aim of minimizing system losses, the pollution index (PI) is calculated based on pollution levels, operation costs, and enhancing voltage levels. In this paper [32], the MCSA has been compared with the Crow search algorithm (CSA), differential evolution (DE), and harmony search algorithm (HSA). The total power losses have been reduced by utilizing the harmony search algorithm (HAS) to allocate the DSTATCOM in the PDG [33]. A multi-objective seeker optimization algorithm (MOSOA) was developed considering the pareto-optimal solution to deduce the final optimal results of DSTATCOM allocation [34]. In addition, the contingency load-loss index (CLLI) has been used to estimate reliability as a planning tool in [34]. The dragonfly algorithm (DA) has been introduced by [35] to allocate the DSTATCOM in PDG. The DA has been validated by a comprehensive analysis with PSO and genetic algorithm (GA). In [36], the improved bacterial foraging search algorithm (IBFA) has been utilized for increasing the bus voltages and stability with minifying the system losses based on the DSTATCOM compensation. Based on [37], the DSTATCOMs have been installed and sized based on the discrete–continuous vortex search algorithm (DCVSA) to minify the energy losses and annual investments. In [38], the MOPSO was utilized to minify the system losses by maximizing the voltage levels and the transmission by ensuring the conditions limits of the node voltage violation and the line loading to allocate the DSTATCOM in DS optimally. The authors in [39] introduced the hybrid analytical–coyote optimization technique (COA) for minifying the power losses and enhancing the voltage levels of the DS based on the DSTATCOM compensation. Under different load conditions, the installation and capacity of the DSTATCOM have been optimized using the Bat Algorithm (BA) [40]. The immune algorithm (IA) was suggested to ensure system power quality, minimize power losses, and reduce the installation price of DSTATCOM in PDG [41]. Noori et al. [42] implements the multi-objective improved golden ratio optimization algorithm (MOIGROM) for the simultaneous allocation of capacitors and DSTATCOM in the

Table 1 The main benefits and applications of DSTATCOM and SVC

Impact on system performance	D-STATCOM	SVC
Load flow control	Good	Good
Voltage control	Best	Best
Transient stability	Better	Good
Dynamic stability	Best	Better
Annual saving	Best	Good
Harmonic resonance sensitivity	Not	High
Dynamic variation range	High	Low
Reactive power generation	High	Low

PDG. Moreover, the power-loss-reduction-factor (PLRF) was used to detect the suggested candidate nodes to locate the capacitors and DSTATCOM in PDGs.

In the second category, the optimum allocation of DSTATCOM with distributed generators (DGs) have been considered. However, the improved PSO was utilized in [43] to allocate the DGs and DSTATCOM in PDG with a focus on the following indexes; voltage profile enhancement Index (VPEI), benefit cost ratio (BCR), and emission cost benefit index (ECBI). In [44], the modified ant lion optimizer (MALO) has been employed to allocate the Photovoltaic DG (PVDG) and DSTATCOM in PDG for minifying the system cost and enhancing the voltage levels (profile/stability). DG and DSTATCOM have been assigned to PDG based on Multi-Objective Functions (MObjF), using several hybrid optimizers, mainly the Firefly Algorithm (FA) via particle swarm optimizations (PSO) [45]. In this research paper [45], the proposed acceleration coefficients for PSO were considered using the following methodologies such as; Adaptive Acceleration Coefficients (FA-AAC-PSO), Autonomous Particle Groups (FA-APG-PSO), Time-Varying Acceleration (FA-TVA-PSO), Nonlinear Dynamic Acceleration Coefficients (FA-NDAC-PSO), and Sine Cosine Acceleration Coefficients (FA-SCAC-PSO).

Table 2 summarizes previous DSTATCOM allocation approaches.

According to Table 2, it is able to note that: (1) most of the objective-functions (ObjFs) have been utilized to analyze the optimum location and capacity of DSTATCOM in power distribution grids (PDGs) focusing on minifying the power/energy losses and enhancing the voltage levels. Not many ObjFs were considered the investment and operating prices. (2) The latest methodologies have presented the investment and operational prices of the DSTATCOM making an allowance for daily demand power graphs into the study. (3) A lot of optimizers have been implemented depending upon the principles of metaheuristic techniques to overcome the problems of DSTATCOM allocations in PDGs and to try ensuring the possibility of escaping from local optimum. In addition, the No-Free-Lunch theory [46] dictates that some mentioned methodologies do not guarantee suitable results in other applications since they remain anchored in the local optimum.

In relation to that, this article proposes an effective algorithm, which combined the Capuchin Search Algorithm (CapSA) [47] with centroid-based fuzzy mutation called mCapSA. mCapSA's main role is to prevent premature convergence of search agents by balancing exploration and exploitation phases without avoiding the immobility of local optimal solutions. The performance of the proposed algorithm is evaluated on CEC'2020 test suite and compared with several optimization algorithms

including; Particle swarm optimization (PSO) [48], Evolution strategy with covariance matrix adaptation (CMA-ES) [49], Gravitational search algorithm (GSA) [50], Whale optimization algorithm (WOA) [51], Harris' Hawks optimization (HHO) [52], Archimedes optimization algorithm (AOA) [53], and the original CapSA. Furthermore, the Wilcoxon sign rank test is used to verify the relevance of the results. Due to the aforementioned and previous reasons, as well as based on specialized literature, the proposed mCapSA is used to locate and demonstrate DSTATCOM optimally in PDGs via the multi-objective function (MObjF) approach. Furthermore, the research paper presents an analytic hierarchy process (AHP) algorithm for selecting weighting factors (WFs) to improve MObjF performance and effectiveness [54, 55]. The advanced scheme is implemented on 33-bus and 118-bus standard systems. The scheme is further applied to a practical model of the power demand of the Middle Egyptian power distribution grid (MEPDG). A 33-bus standard system is used to model the power demand of the MEPDG. Furthermore, it has been implemented a comprehensive study that applied on 33-bus and 118-bus standard PDG between the proposed approach (mCapSA) with its original one and with other recent optimizers in the literature such as basic particle swarm optimizer (PSO) [45], basic Firefly Algorithm (FA) [45], hybrid FA-PSO [45], FA-Sine Cosine Acceleration Coefficients-PSO (FA-SCAC-PSO), FA-Nonlinear Dynamic Acceleration Coefficients-PSO (FA-NDAC-PSO) [45], FA-Adaptive Acceleration Coefficients-PSO (FA-AAC-PSO) [45], FA-Autonomous Particles Groups-PSO (FA-APG-PSO) [45], and FA-Time-Varying Acceleration-PSO (FA-TVA-PSO) [45], bacterial foraging optimization algorithm (BFOA) [28], multi-objective PSO (MOPSO) [42], multi-objective golden ratio optimization method (MOGROM) [42], and the improved one of MOGROM named (MOIGROM) [42]. However, the main contributions are summarized as follows:

- Developing an effective optimization called mCapSA to enhance the performance of the original CapSA.
- The performance of the mCapSA is legalized based on the CEC'2020 test suite.
- The analytical hierarchy process (AHP) algorithm is utilized to elect the most suitable weighting factors (WFs) to enhance the multi-objective function (MObjF) performance and effectivity via mCapSA optimizer process.
- Sufficient comprehensive analysis is executed between the efficient mCapSa and 7 recent optimizers considering the original one.

Table 2 Applied approaches for DSTATCOM placement techniques

Method	Objective function	Approach discussion	Test systems	Demerits	References
Modal analysis	Power loss and voltage profile	Voltage profile and power losses were examined after and before DSTATCOM devices were placed	33-bus DS	A comparison was not conducted between the numerical results and those obtained using other optimization algorithms and techniques to validate the proposed method	[18]
				There was no consideration given to the large-scale system of the network in the study	
Analytical methods	Power loss and voltage profile	DSTATCOM is modeled to determine the optimal size to maintain a voltage magnitude of 1 p.u. at the node where it is connected, as well as to supply the reactive power for compensation	33-bus DS	A comparison was not conducted between the numerical results and those obtained using other optimization algorithms and techniques to validate the proposed method	[19]
				There was no consideration given to the large-scale system of the network in the study	
				The objective function is limited to improving the voltage profile	
	Loss relief, PLI	Power loss is calculated using load flow methods, and the node with the greatest PLI value is perfectly suited for the DSTATCOM installation	UK 38-bus practical DS	A comparison was not conducted between the numerical results and those obtained using other optimization algorithms and techniques to validate the proposed method	[20]
				There was no consideration given to the large-scale system of the network in the study	
				The objective function is limited to power losses minimization	
	VSI	The authors employed VSI to determine the best location for DSTATCOM	12, 34, and 69-bus DS	Statistical assessment for the competitive algorithms, higher bus and real-time radial distribution systems haven't considered	[21]
				A comparison was not conducted between the numerical results and those obtained using other optimization algorithms and techniques to validate the proposed method	
	Power loss and voltage profile	Voltage profile and power losses were examined after and before these devices were placed. It has been considered the SI and PLI to develop the allocation of DSTATCOM	33-bus DS	A comparison was not conducted between the numerical results and those obtained using other optimization algorithms and techniques to validate the proposed method	[22]
				The study neglected the operating cost of the system	

Table 2 (continued)

Method	Objective function	Approach discussion	Test systems	Demerits	References
	Power loss, voltage profile, and energy saving	Using VSI and PLI approaches to determine D-STATCOM placement in PDG. The D-STATCOM capacity has been developed based on the variational technique for PDG	33-bus DS	A limited objective functions were used based on minimizing the system losses	[23]
				It was observed that the proposed scheme was not guaranteed to be globally optimal based on the comparison of the numerical results with other optimization algorithms	
				The study neglected the operating cost of the system	
	VSI, pollution index (PI), power loss, and economic index (EI)	The authors' work includes a number of sensitivity indices for determining the most advantageous DSTATCOM selection	51-Bus DS	The trend of the objective function with the number of iterations has not been considered to illustrate at what iteration reaching to the optimal solutions. Statistical assessment for the competitive algorithms, higher bus and real-time radial distribution systems haven't considered	[24]
	Active power loss, and VSI	The proposed technique relies heavily on VSI and active power loss. The MCS approach was used to correct for load variations	33-bus and 94-bus PDG	The author compared the numerical results with only one optimization algorithm to validate the proposed scheme, which is not enough. Statistical analysis of competitive algorithms, higher bus, and real-time radial distribution systems has not been carried out	[25]
	VSI, and LSF	For DSTATCOM allocation, PLI and VSI are employed as ObjF indices	33 bus PDG	A limited objective functions were used based on minimizing the system losses	[26]
				There was no consideration given to the large-scale system of the network in the study	
				Statistical analysis of competitive algorithms, higher bus, and real-time radial distribution systems has not been carried out	
Optimization techniques	Total power loss along with enhancing voltage profile	PSO is employed for the concurrent allocation of DSTATCOM and DG problems for voltage profile augmentation and power loss minimization	12, 34, and 69-bus PDG	limited objective functions were used based on minimizing the system losses and voltage deviation	[27]
				Statistical analysis of competitive algorithms, higher bus, and real-time radial distribution systems has not been carried out	
	Total power loss along with voltage profile and total operational cost	BFOA was employed to tackle the DSTATCOM and DG allocation problems in PDG using a multi-objective function	33-bus and 119-bus DS	Statistical analysis of competitive algorithms, higher bus, and real-time radial distribution systems has not been carried out	[28]

Table 2 (continued)

Method	Objective function	Approach discussion	Test systems	Demerits	References
	Total power loss along with voltage deviation	The candidate allocation of DSTATCOM for the system's power loss lessening has been solved by using the EBA method	69-bus PDG	Limited objective functions were used based on minimizing the system losses and voltage deviation. Statistical analysis of competitive algorithms, higher bus, and real-time radial distribution systems has not been carried out	[29]
	Total installation/operational prices and THD	In DS, the MOGA approach is employed for ObjFs such as THD and total construction costs	33-bus DS	The study neglected the operating cost of the system Statistical analysis of competitive algorithms, higher bus, and real-time radial distribution systems has not been carried out There was no consideration given to the large-scale system of the network in the study	[30]
	Energy price, TNP, and the annual saving price	DE with a backward-forward sweep is utilized for load flow in DS, and when compared to another methodologies, the DE approach provides less CPU time, less power loss, a lot of ObjF, and the highest TNP	30, 33, and 69-bus DS	The study neglected the operating cost of the system Statistical analysis of competitive algorithms, higher bus, and real-time radial distribution systems has not been carried out	[31]
	Line losses, VSI, PI, and improvement in financial benefits	MCSA's control restrictions were logically modified by making them adaptable with iterations at various loading levels. The suggested algorithm is evaluated in comparison to the CSA, HSA, and DE algorithms	51-Bus DS	The study neglected the operating cost of the system There was no consideration given to the large-scale system of the network in the study	[32]
	Total power losses lessening	The HSA is used to determine the best position and size of DSTATCOM	33-Bus DS	A limited objective functions were used based on minimizing the system losses The author compared the numerical results with only one optimization algorithm to validate the proposed scheme, which is not enough. Statistical analysis of competitive algorithms, higher bus, and real-time radial distribution systems has not been carried out There was no consideration given to the large-scale system of the network in the study	[33]

Table 2 (continued)

Method	Objective function	Approach discussion	Test systems	Demerits	References
	Voltage profile control	The MOSOA algorithm was utilized for placement with a Pareto-optimal solution, and the results were compared to the NSGA-II technique for DS planning	54-bus DS	The variable load models and hourly load variation haven't been considered	[34]
				The author compared the numerical results with only one optimization algorithm to validate the proposed scheme, which is not enough	
				The study neglected the operating cost of the system	
				There was no consideration given to the large-scale system of the network in the study	
	Voltage levels and power loss index	In terms of cost analysis and convergence speed, the novel swarm astuteness-based DA model is compared to PSO and GA	33-bus DS	A comparison was not conducted between the numerical results and those obtained using other optimization algorithms and techniques to validate the proposed method	[35]
				There was no consideration given to the large-scale system of the network in the study	
				The objective function is limited. Statistical assessment for the competitive algorithms, higher bus and real-time radial distribution systems haven't considered	
	Minimization of ILR, maximization of IVPE, and minimization of IPR	Maximizing system rewards through optimal positioning of DG and DSTATCOM considering load changings	33-Bus and 69-bus DS	The study neglected the operating cost of the system	[43]
				Statistical analysis of competitive algorithms, higher bus, and real-time radial distribution systems has not been carried out	
	Minify power losses and enhance stability and profile levels	Improved IBFA is employed for sizing and placing the DSTATCOM in the distribution sector	Practical Quha feeder of 78-buse of Lachi's PDG of Ethiopia	The author compared the numerical results with only one optimization algorithm to validate the proposed scheme, which is not enough	[36]
				The study neglected the operating costs of the system	
				Statistical analysis of competitive algorithms, higher bus, and real-time radial distribution systems has not been carried out	
	Minify energy losses and annum investments prices	DCVSA has been employed, where, the DSTATCOMs were installed at the nodes evaluated by the discrete portion of the codification, while continuous portion determined their optimum capacity	33-Bus and 69-bus DS	A comparison was not conducted between the numerical results and those obtained using other optimization algorithms and techniques to validate the proposed method	[37]
				The study neglected the operating cost of the system	

Table 2 (continued)

Method	Objective function	Approach discussion	Test systems	Demerits	References
				Statistical analysis of competitive algorithms, higher bus, and real-time radial distribution systems has not been carried out	
	Minify system losses and enhance voltage levels with the transmitted power	MOPSO methodology has been proposed to find the optimal solutions for allocate the DSTATCOM with the reconfiguration of the power network at the same time	33-Bus and 69-bus DS	A comparison was not conducted between the numerical results and those obtained using other optimization algorithms and techniques to validate the proposed method	[38]
				The study neglected the operating cost of the system	
				Statistical analysis of competitive algorithms, higher bus, and real-time radial distribution systems has not been carried out	
	Active power losses minimization and voltage profile improvement	Hybrid analytical–COA has been proposed, where the DSTATCOMs were located at the buses determining by the COA method, while the analytical algorithm evaluated their optimum capacity	33-Bus and 69-bus DS	A very limited objective functions were used based on minimizing the system losses	[39]
				The analytical technique is used to determine the proper sizes of DSTATCOMs, while the COA is used to specify the locations into RDS	
				The work focused on minimizing the total system losses without caring about the efficient improvement in the voltage profile according to the comparisons between other algorithms	
				Global optimality was not guaranteed	
				Statistical analysis of competitive algorithms, higher bus, and real-time radial distribution systems has not been carried out	
	Reducing the system power losses	VSI is performed to search the best placement for locating the DSTATCOM. The size of the DSTATCOM was evaluated optimally by proposing the BA	33-Bus and 69-bus DS	A limited objective functions were used based on minimizing the system losses	[40]
				The study neglected the operating cost of the system	
				Statistical analysis of competitive algorithms, higher bus, and real-time radial distribution systems has not been carried out	
	Minify power losses and annum investments prices	IA technique was proposed to find the place and size of the DSTATCOM	33-Bus and 69-bus DS	A comparison was not conducted between the numerical results and those obtained using other optimization algorithms and techniques to validate the proposed method	[41]

Table 2 (continued)

Method	Objective function	Approach discussion	Test systems	Demerits	References
	Minify the cost index, voltage deviation index (VDI), and maximize the VSI	MALO has been suggested to minimize the multi-objective function based on the optimal management of PVDG and DSTATCOM in PDG	69-Bus and 118-bus DS	The author compared the numerical results with only one optimization algorithm to validate the proposed scheme, which is not enough. Statistical assessment for the competitive algorithms hasn't presented	[44]
	Power losses, short circuit, voltage deviation, net saving, as well as environmental pollution reduction	FA-SCAC-PSO has been proposed to allocate the PVDG and DSTATCOM in PDG. In addition, a comprehensive analysis was implemented between numerous acceleration coefficients for PSO considering various hybrid methodologies-based FA	33-Bus and 69-bus DS. In addition to the practical 205-bus Algerian DS	The variable load models, hourly variation of DG power-based PV and WT renewable sources, and the installation costs of DG and DSTATCOM systems haven't been considered (i.e., the effect of DSTATCOM has not been considered/studied clearly)	[45]
	Minify power losses, annum investments prices, and voltage deviations	MOIGROM has been employed to allocate capacitors and DSTATCOM considering different scenarios as separately location for each device and simultaneously in various PDGs	13-Bus, 69-bus, and 118-bus PDGs	A very limited objective functions were used based on minimizing the system losses Statistical assessment for the competitive algorithms hasn't presented	[42]

- The performance of the proposed approach is compared with several other optimization algorithms in the literature which solved the same problem.
- An application of real-time measurements of the power load curve of the middle Egyptian distribution grid was conducted on the 33-bus grid, to determine the efficiency and validity of the proposed scheme.

The following structure of the manuscript is divided as: Sect. 2 introduces the mathematical scheme formulation. Section 3 defines the basic concept of CapSA. In Sect. 4, the implementation of the mCapSA algorithm is introduced. The performance estimation of mCapSA is explained in Sect. 5. The simulation findings as well as commentaries are drawn in Sect. 6. Finally, Sect. 7 deduces the conclusions.

2 Mathematical scheme formulation

Over the last 2 decades, the growing utilization of renewable energy-based distributed generators (DG) in the grid along with rapid demand growth has generated new problems for utilities in terms of voltage stability, power quality, and effective energy utilization. As a result, paying close attention to DSTACOMs' technology has become a critical issue that must be considered for its impact on the distribution system (DS). It has become essential to determine the most appropriate allocation of DSTACOMs to address these issues. This is because they constitute the main issue under network constraints, including load flow, with the purpose of enhancing overall system performance. Figure 1 presents a sample distribution network considering the DSTATCOM connection.

This paper uses the Backward-forward sweep method (BFSM) as an alternative to standard approaches to load flow reckoning due to the low X/R ratio, imbalanced load, and radially laid-out nature of PDG [2, 56].

2.1 Modelling of DSTATCOM

The DSTATCOM device is considered to be a device related to FACTs. At a point of common coupling (PCC), DSTATCOM can absorb/inject the reactive currents. As illustrated by Fig. 1, the DSTATCOM device can be connected to the selected bus based on an optimization algorithm with the optimum capacity. In DSTATCOM device, the voltage amplitude and its angle are regulated based on the PID controller controlling the node voltage and to enhance the power factor (PF) [11]. DSTATCOM can either produce or consume the reactive power that undergoes in this manuscript. The phasor diagram after
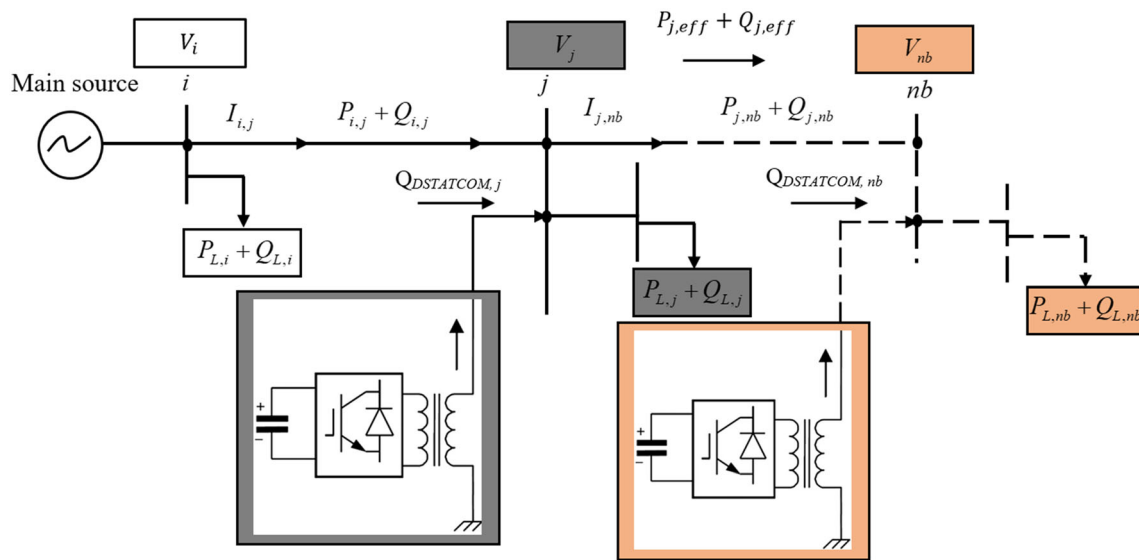
Fig. 1 The distribution grid sample including DSTATCOM

DSTATCOM integration is presented by [41]. Moreover, the reactive power exchanged with the grid at node i are estimated by the equations in [45]. However, the reactive power injected by DSTATCOM is computed as in the following formula,

$$Q_{\text{DSTATCOM},i} = V_{\text{new},i} \cdot I_{\text{DSTATCOM}} \tag{1}$$

$$I_{\text{DSTATCOM}} = |I_{\text{DSTATCOM}}| \angle \left(\theta_{\text{new}} + \frac{\pi}{2} \right) \tag{2}$$

$$V_{\text{new},i} = |V_{\text{new},i}| \angle \theta_{\text{new}} \tag{3}$$

where $|V_{\text{new},i}|$ is the absolute voltage at node i

2.2 multi-objective function (MObjF) approach

In the proposed work, the suggested MObjF approach is implemented including the objective function of power losses (ObjF$_1$), voltage deviation (ObjF$_2$), voltage stability (ObjF$_3$), and the capital annual price (ObjF$_4$) that can be evaluated in the following formula,

$$\text{MObjF} = \kappa_1 \text{ObjF}_1 + \kappa_2 \text{ObjF}_2 + \kappa_3 \text{ObjF}_3 + \kappa_4 \text{ObjF}_4 \tag{4}$$

where the κ_1, κ_2, κ_3, and κ_4 are the weighting factors and they have been determined in this paper using AHP method that is explained in Sect. 2.4.

Based on Fig. 1, the power losses, which are active $P_{\text{Loss}(i,j)}$ and reactive $Q_{\text{Loss}(i,j)}$, through "i-bus" and "j-bus" are estimated by the following equations,

$$P_{\text{Loss}(i,j)} = R_{i,j} \frac{\left(P_{i,j}^2 + Q_{i,j}^2 \right)}{V_i^2} \tag{5}$$

$$Q_{\text{Loss}(i,j)} = X_{i,j} \frac{\left(P_{i,j}^2 + Q_{i,j}^2 \right)}{V_i^2} \tag{6}$$

wherever, V_i is the voltage at i-bus, R and X are the resistance and reactance of the branch, respectively.

The total basic active power loss of PDGs is evaluated as,

$$P_{\text{TLoss},b} = \sum_{j=1}^{N} P_{\text{Loss}(i,j)} \tag{7}$$

wherever, N is the branches number.

Hence, the ObjF$_1$ is evaluated as a proportion of the system active losses including DSTATCOMs ($P_{\text{DST,TLoss}}$) to the basic one with no DSTATCOMs as follows,

$$\text{ObjF}_1 = \frac{P_{\text{DST,TLoss}}}{P_{\text{TLoss},b}} \tag{8}$$

The ObjF$_2$ approach is formulated as follows:

The index of the voltage deviation at the basic-scenario (IVD$_b$) without DSTATCOMs is formulated as follows,

$$\begin{aligned} \text{IVD}_b = \sum_{i=2}^{nb} \Big[& \left((V_{\max} - V_{i,b})/(V_{\max} - V_{\min}) \right)^2 \\ & - \left((V_{i,b} - V_{\min})/(V_{\max} - V_{\min}) \right)^2 \Big] \end{aligned} \tag{9}$$

The index of the voltage deviation with DSTATCOM location (IVD$_{\text{DST}}$) can be written as follows,

$$\begin{aligned} \text{IVD}_{\text{DST}} = \sum_{i=2}^{nb} \Big[&\big((V_{\max} - V_{i,\text{DST}})/(V_{\max} - V_{\min})\big)^2 \\ &- \big((V_{i,\text{DST}} - V_{\min})/(V_{\max} - V_{\min})\big)^2 \Big] \end{aligned} \tag{10}$$

where the voltage boundaries $V_{\max}$ and $V_{\min}$ are deemed to be 1.05 p.u. and 0.95 p.u, and the 'nb' represents the node number. Consequently, the ObjF_2 is realized to be the ratio between the difference of the base index and the index with DSTATCOM allocation to the base one as follows,

$$\text{ObjF}_2 = \frac{\text{IVD}_b}{\text{IVD}_{\text{DST}} + \text{IVD}_b} \tag{11}$$

The main purpose of the voltage stability (VS) evaluation is to inspect the level of system security. Based on the power flow determination, the VS of network nodes can be maximized while avoiding voltage collapse potential. The VS is deduced from Fig. 1 as follows,

$$\begin{aligned} \text{VS}_{(j)} = |V_i|^4 &- 4 \times [P_{j,\text{eff}} \times X_{ij} - Q_{j,\text{eff}} \times R_{ij}]^2 \\ &- 4 \times [P_{j,\text{eff}} \times R_{ij} - Q_{j,\text{eff}} \times X_{ij}] \times |V_i|^2 \end{aligned} \tag{12}$$

where the $P_{j,\text{eff}}$ and $Q_{j,\text{eff}}$ are the effective values of active and reactive loads, consequently, that are beyond jth-bus.

Regarding the VS estimation, the ObjF_3 is the ratio of the voltage stability deviation in the base case to the difference between the base index and the index with DSTATCOM integration as follows:

The Index of the voltage stability deviation at the basic scenario (IVSD_b) with no DSTATCOM can be expressed by,

$$\text{IVSD}_b = \sum_{i=2}^{nb} \Big[\big((1/\text{VS}_{\max}) - (1/\text{VS}_{i,b})\big)^2 \Big] \tag{13}$$

On the other hand, the Index of the voltage stability deviation with DSTATCOM (IVSD_{DST}) can be deduced by,

$$\text{IVSD}_{\text{DST}} = \sum_{i=2}^{nb} \Big[\big((1/\text{VS}_{\max}) - (1/\text{VS}_{i,\text{DST}})\big)^2 \Big] \tag{14}$$

Finally, the ObjF_3 is given as follows,

$$\text{ObjF}_3 = \frac{\text{IVSD}_{,b}}{\text{IVSD}_{\text{DST}} + \text{IVSD}_{,b}} \tag{15}$$

The capital annual price (CAP_t) of the proposed scheme as ObjF_4 is made up two parts as follows:

(I) the first part is the energy price after allocating the DSTATCOM can be rewritten in the following formula,

$$\text{En}_{\text{DST}} = \sum_{t_r=1}^{T_p} (\text{PWF})^{t_r} \cdot C_{\text{en}} \cdot P_{\text{DST,TLoss}} \cdot T_h \tag{16}$$

where C_{en} is the coefficient of the energy price rate (60 \$/

MWh) [45], T_p is the scheduling period of years ($T_p = 30$ years), t_r is years' number, T_h can be considered as the hour/year. Equation (17) gives the present-worth-factor (PWF) by the following formula,

$$\text{PWF} = \frac{1 + \text{InfR}}{1 + \text{IntR}} \tag{17}$$

wherever, the inflation (InfR) and interest (IntR) equal 9% and 12.5%, respectively [2].

On the other hand, the energy price in the base scenario with no DSTATCOM location and it can be estimated by the following equation,

$$\text{En}_b = \sum_{t_r=1}^{T_p} (\text{PWF})^{t_r} \cdot C_{\text{en}} \cdot P_{\text{TLoss,b}} \cdot T_h \tag{18}$$

(II) the second part is formulated to include the total operational and location costs of the DSTATCOM (TOL_{DST}) can be formulated by the following:

$$\begin{aligned} \text{TOL}_{\text{DST}} = \sum_{i=1}^{n_{\text{LL}}} \lambda_i \Bigg[&\sum_{i=1}^{n_{\text{DST}}} Q_{\text{DSTATCOM},i} \\ &\times \frac{(1+\alpha)^{T_{\text{DST}} \times \alpha}}{(1+\alpha)^{T_{\text{DST}}} - 1} \times \beta_{\text{DST}} + \sum_{i=1}^{n_{\text{DST}}} D_i \times \beta_{\text{Loc}} \Bigg] \end{aligned} \tag{19}$$

where $\alpha = 0.1$ that represents the expected rate of return and T_{DST} is the longevity of the DSTATCOM [41]. The β_{DST} is the operational cost of the Q_{DSTATCOM} ($\beta_{\text{DST}} = 5.3$ \$/kVAR) [42]. D_i is the number of DSTATCOM locations. The β_{Loc} is the investment price of the Q_{DSTATCOM} location ($\beta_{\text{Loc}} = 1600$ \$/location) [42]. The n_{DST} is the DSTATCOM number. T_y is the time period based on the ith load level (LL). The n_{LL} is the number of the LL. The λ_i is the ratio of the period of the ith LL to the full time period and it can be evaluated as follows [41],

$$\lambda_i = \begin{cases} 1; & \text{if } \text{LL} = 0 \\ \dfrac{T_{y_i}}{\sum\limits_{i=1}^{n_{\text{LL}}} T_{y_i}}; & \text{if } \text{LL} > 1 \end{cases} \tag{20}$$

Then, the ObjF_4 can be estimated as the ratio of CAP_t by the following equation,

$$\text{ObjF}_4 = \frac{\text{En}_b}{(\text{En}_{\text{DST}} + \text{TOL}_{\text{DST}}) + \text{En}_b} = \frac{\text{CAP}_{t,b}}{\text{CAP}_{t,\text{DST}} + \text{CAP}_{t,b}} \tag{21}$$

2.3 Constraints

The limitations that assure stellar performance of the proposed system can be deduced as follows:

- Power balance constraints can be written according to Fig. 1 as follows,

$$P_j = P_{i,j} - P_{L,j} - R_{i,j}\frac{\left(P_{i,j}^2 + Q_{i,j}^2\right)}{V_i^2} \tag{22}$$

$$Q_j = Q_{i,j} - Q_{L,j} - X_{i,j}\frac{\left(P_{i,j}^2 + Q_{i,j}^2\right)}{V_i^2} + \left(\psi_{\text{DST}} \times Q_{\text{DSTATCOM},j}\right) \tag{23}$$

where the Ψ_{DST} is the reactive power set 0 or 1.

- Voltage profile level,

$$\left|V_i^{\min}\right| \le |V_i| \le \left|V_i^{\max}\right|, \ \forall i \in nb \tag{24}$$

- DSTATCOM size,

$$Q_{\text{DSTATCOM}}^{\min} \le Q_{\text{DSTATCOM}} \le Q_{\text{DSTATCOM}}^{\max} \tag{25}$$

- DSTATCOM location,

$$2 \le \text{DSTATCOM}_{\text{Location}} \le nb \tag{26}$$

2.4 AHP method for weighting factors assignment

Adding weights to each objective function (ObjF) may enhance the performance of the current scheme. The prepared AHP algorithm is the suitable tool to deduce the optimum weights for the specific objective [54, 55]. The AHP constructions, steps, and definitions can be deduced by [54, 55]. However, to start with the AHP method, it is required to construct the reciprocal matrix [A] based upon the decision maker's pairwise comparison in the range of 1–9. As mentioned by [55], in the first step, a pairwise comparison matrix is formed on a scale from 1 to 9 by comparing the importance of each of the indices. (Therefore in the current manuscript, indices refer to objectives.) The larger the scale value, the more important the index is. In this paper, it is therefore the power losses that are of the utmost importance, followed by the voltage level, voltage stability, and the annual total cost. In this case, the weighting factor of power losses will be the highest, followed by the weighting factors of voltage level, voltage stability, and the annual total cost.

However, the [A] matrix size can be estimated considering the elected Number of objective functions (NF). The individual ObjF can be represented as a row, where the element higher value of such row specifies the significance of such ObjF versus the other one. Equation (27) estimated the square matrix [A] as follows [54, 55],

$$A = \begin{bmatrix} a_{ii} & a_{ij} & . & . & a_{iNF} \\ 1/a_{ji} & a_{jj} & . & . & a_{jNF} \\ . & . & . & . & . \\ . & . & . & . & . \\ 1/a_{NFi} & 1/a_{NFj} & . & . & a_{NFNF} \end{bmatrix} \tag{27}$$

where a_{ii} equals unity representing the self-value that is dedicated to objective i. The mutual value $a_{ij} = 1/a_{ji}$ sets to objective j in contrast to objective i. The variables i and j ε [1, NF].

However, the weighting-factors (WFs) for each objective i is determined using the following Eq. (28),

$$\kappa_i = \frac{\sqrt[\text{NF}]{\prod_{j=1}^{\text{NF}} a_{ij}}}{\sum_{i=1}^{\text{NF}} \sqrt[\text{NF}]{\prod_{j=1}^{\text{NF}} a_{ij}}} \tag{28}$$

where the WFs is introduced in as a vector in the following form $\kappa = [\kappa_1, \kappa_2, \ldots, \kappa_{NF}]^{\text{T}}$.

Finally, the consistency of the matrix [A] can be verified based on the index of consistency ratio (I_{CR}) as follows,

$$I_{\text{CR}} = \frac{I_{\text{CI}}}{I_{\text{RI}}} < 0.1; \quad \text{where} \quad I_{\text{CI}} = \frac{(\lambda_{\max} - \text{NF})}{(\text{NF} - 1)} \tag{29}$$

where I_{CI} and I_{RI} are the consistency and random indexes, correspondingly. In the case of the I_{CR} is below 0.1 p.u., then, the weight of each index is sensible. The value of the random index, I_{RI} depends upon the NF as well as these values are found by Table 3 [54, 55].

The maximum eigenvalue ($\lambda_{\max}$) can be evaluated by the following form,

$$[A][W] = \lambda_{\max}[W] \tag{30}$$

2.5 Sensitivity index algorithm (SIA)

In Fig. 1, the line active losses ($P_{\text{line}(i,j)}$) can be defined based on the effective values of active and reactive loads $P_{j,\text{eff}} + Q_{j,\text{eff}}$, consequently, that are behind jth bus by the following Eq. (31),

$$P_{\text{line}(i,j)} = R_{ij}\frac{\left(P_{j,\text{eff}}^2 + jQ_{j,\text{eff}}^2\right)}{V_j^2} \tag{31}$$

Table 3 Random index (I_{RI}) values

NF	1	2	3	4	5	6	7	8	9
I_{RI}	0.00	0.00	0.58	0.90	1.12	1.24	1.32	1.41	1.45

Henceforward, the first derivative of Eq. (31) according to the $P_{j,\text{eff}}$ is defined as the Sensitivity Index of Losses (SIL) that is expressed by Eq. (32) [2],

$$\text{SIL}_{(i,j)} = \frac{2 \cdot P_{j,\text{eff}} \cdot R_{ij}}{V_j^2} \tag{32}$$

The existing values of the SIL are arranged based on the voltage stability index (VSI) values that are given by Eq. (12) from high to low in descendant order for all lines. As a means of reducing the research space for the proposed techniques, it will be selected (2/3) as a candidate node from the existing results of the SIA method to deduce the most optimal values.

3 Capuchin search algorithm (CapSA)

This section presents the design of Capuchin search algorithm (CapSA), which can focus on the attitude of the capuchin monkeys as a major social model of animals seeking food, in detail [47]. As follows, CapSA consists of three main stages: Leaping motion (global search), Swinging motion (local search) and Climbing motion (local search):

3.1 Stage 1: Leaping motion

The leaping motion considering the jumping strategy is comparable to the global search. The actual distance stimulated by the capuchin outfits the horizontal distance, x, among the source tree branch and the target tree. Mathematically, the third law of motion can be utilized to define the x as follows,

$$x = x_o + vt + \frac{1}{2}at^2 \tag{33}$$

where x and x_0 are the new and initial positions of the capuchin. The v and v_0 are the velocity and the initial one of the capuchins. The a is the acceleration, and t can be defined as the time instance.

The v during the jumping motion is defined based up on the first law of motion as follows,

$$v = v_0 + at \tag{34}$$

3.2 Swinging motion

This movement approach can be simulated a local search procedure, which is presented by two models. Consistent with the trigonometry rules, the x throughout the swinging motion of the capuchin is identified by Eq. (35),

$$x = l \sin \theta \tag{35}$$

where θ is the angle.

3.3 Climbing motion

This climbing motion is termed by means of a demonstrative and a theoretical model. The capuchin position throughout the climbing or sliding a tree is evaluated via Eqs. (33) and (34) as follows,

$$x = x_0 + v_0 t + \frac{1}{2}(v_f - v_0)t^2 \tag{36}$$

where $t = 1$, which is the iteration to identify the inconsistency between iterations.

3.4 Arithmetical concept of CapSA

Like other swarm intelligence methodologies, the CapSA method is defined as a population-based technique, which can initialize a number of the established particles in advance in a random form. It is imperative to note that the singulars in capuchins' swarms have two diversities: Leader (i.e., Alpha) and supporters. However, Eq. (37) is performed to assign the initial position of each capuchin in the swarm as follows,

$$x^i = ub_j + r \times (ub_j - lb_j) \tag{37}$$

where ub_j and lb_j are the higher and minor bounds of the ith capuchin in the jth dimension, correspondingly. $r \in [0, 1]$ is a random number.

CapSA's population is constructed by including both individuals—the alpha of the team, as well as its followers. However, the location of leader capuchins is defined by the following formula,

$$x = F_j + \frac{P_{bf}(vj)^{i2}\sin(2\theta)}{g} \tag{38}$$
$$i < n/2; 0.1 < \epsilon \le 0.20$$

The jumping angle of the capuchins θ is formulated as,

$$\theta = \frac{3}{2}r \tag{39}$$

In the CapSA methodology process, for the duration global and local search implementation, the τ is responsible to realize a balance between exploration and exploitation. This τ factor is defined by Eq. (40),

$$\tau = \beta_0 e^{-\beta_1 \left(\frac{k}{k}\right)^{\beta_2}} \tag{40}$$

where k/K represent the current/maximum iteration values. The factors β_0, β_1 and β_2 are arbitrarily designated as 2, 21, and 2.

The velocity of the CapSA is estimated using the following formula,

Table 4 Parameter setting of mCapSA and the counterparts

Algorithms	Variables
Common settings	Search Agents number = 30
	FEs = 100,000
	Independent runs are 30
	Dimensions (Dim) is 10
PSO	Cognitive component = 1.8 Social component = 1.8 Inertia weight = 0.6
CMA-ES	alpha_{mu} = 2
GSA	$\alpha = 20$, G0 = 100, Rnorm = 2, Rpower = 1
WOA	α, variable decreases linearly from 2 to 0
	a2, linearly decreases from -1 to -2
HHO	E0 $\in [-1, 1]$, $\beta = 1.5$
AOA	C1 = 2, C2 = 6, $u = .9$, $l = .1$
CapSA and mCapSA	P_{bf} and P_{ef} equal 7 and 9

$$v_j^i = pv_j^i + \tau a_1\left(xi_{bestes}^i - x_j^i\right)r_1 + \tau a_2\left(fj_j - x_j^i\right) \quad (41)$$

The updated location of the alpha and the followers' capuchins is deduced by follows,

$$x_i^j = fj_j + \frac{P_{ef}P_{bf}\left(v_j^i\right)^2 \sin(2\theta)}{g}, i < \frac{n}{2}; 0.2 < \epsilon \leq 0.30 \quad (42)$$

where P_{bf} and P_{ef} are the balance and elasticity factors' probability of the capuchin motion on the ground. Hence, the updated location of leader capuchins that utilize normal walking is defined by the following Eq. (43),

$$x_j^i = x_j^i + v_j^i, \qquad i < \frac{n}{20}.3 < \epsilon \leq 0.50 \quad (43)$$

The two P_{bf} and P_{ef} factors are responsible for the efficient exploitation and exploration to boost the competence of the local as well as the global search strategy. The estimated values of these factors are $P_{bf} = 0.7$ and $P_{ef} = 9$ that have been deduced by intensive analysis.

Some of the capuchins are swinging on branches by strolling over not large distances, where the leader and followers may consider a local search for seeking foods on as well as around the tree branches. These capuchins utilize two processes, using tails to clutch on a tree branch as well as using the swing process to detect the food sources on the other side of the branch. Hence, the capuchins' location is estimated by Eq. (44) as follows,

$$x_j^i = fi + P_{bf} \times \sin(2\theta), \qquad i < \frac{n}{2}; 0.5 < \epsilon \leq 0.75 \quad (44)$$

Some of the capuchins are climbing on the trees and branches numerous times throughout foraging in a process similar to local search. Therefore, the capuchins' location is estimated by Eq. (45) as follows

$$x_j^i = F_j + tP_{bf}\left(v_j^i - v_{j-1}^i\right), \qquad i < \frac{n}{2; 0.75} < \epsilon \leq 1.0 \quad (45)$$

where v_j^i represents the velocity of the ith capuchin in the jth dimension in a current form. On the other hand, the v_{j-1}^i introduces the previous velocity.

In some random conditions of the capuchins reposition, the capuchins may execute new different ways to deduce a better way for seeking the food source. The mention attitude can be realized to allow the capuchins enhancing their exploration professionally of the forest to evaluate new regions for food sources. During foraging, these random repositions are expressed using the following Eq. (46).

$$x_i^j = t \times \left[lb_j + \epsilon \times \left(ub_j - lb_j\right)\right], \qquad i < n/2; \epsilon \leq \text{Pr} \quad (46)$$

where the constant Pr = 0.1 represents the possibility of random search of the capuchins.

During the iteration process of the optimizer, the variance among successive iterations, $t_i - t_{i-1}$, is equal to 1. Hence, the attitude of the accompanying capuchins following the alphas, can be deduced as follows,

$$x_j^i = \frac{\frac{1}{2}\left(x_j^i + x_j^{i-1}\right)n}{2} \leq i \leq n \quad (47)$$

4 Modified capuchin search algorithm (CapSA)

In the current section, the prepared mCapSA technique is detailed as well as how it boosts search capabilities and balances the exploration and exploitation phases. This is compared with the original CapSA. The proposed fuzzy mutation embedded in the capuchin search algorithm. While CapSA is an efficient meta-heuristic algorithm, it
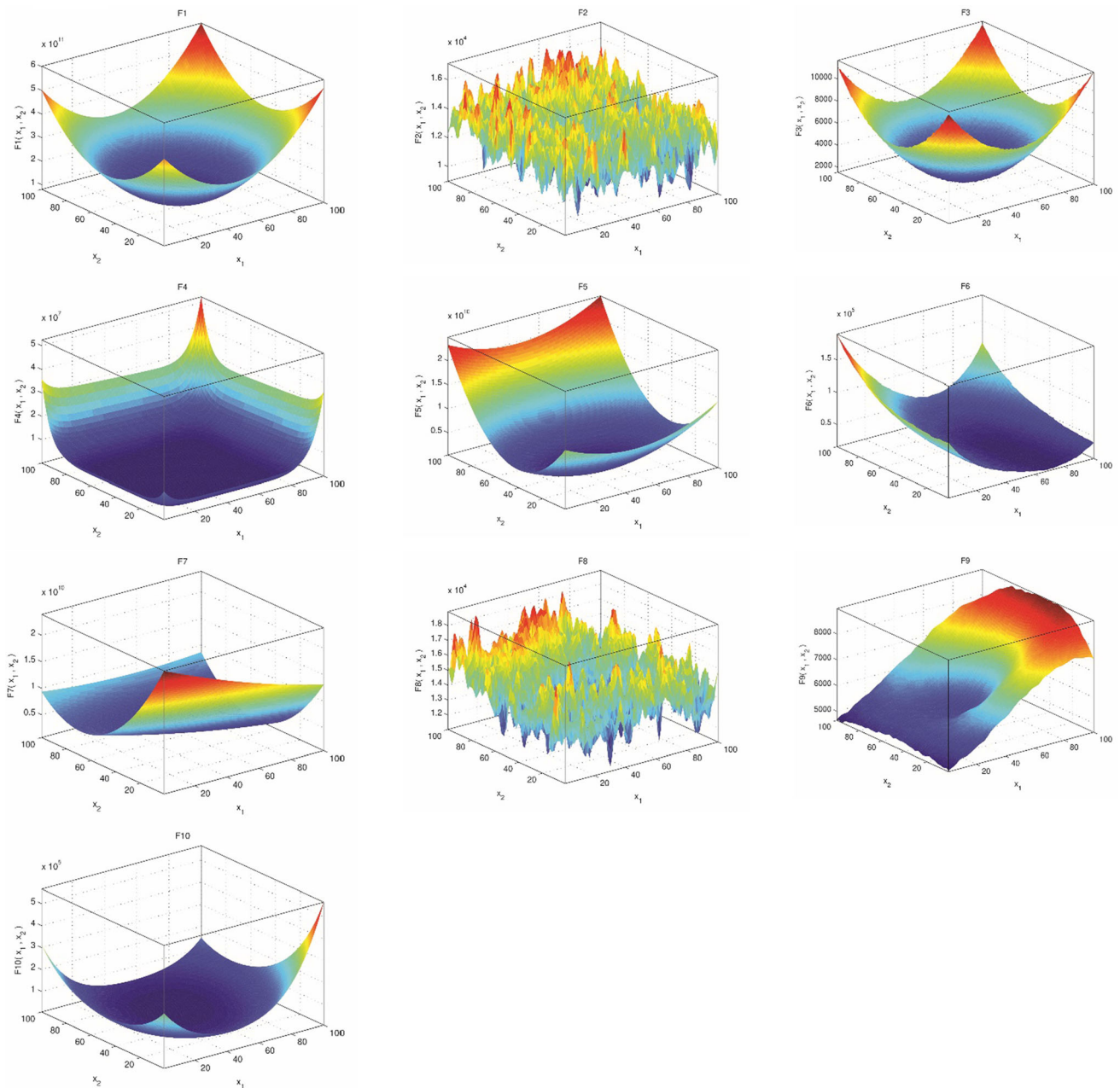
Fig. 2 The 2D visualization of the CEC'2020 benchmark functions

suffers from local optimum stagnation and low convergence rate, as do many classical meta-heuristic algorithms. CapSA may occasionally be affected by premature convergence, skipping of the real solution, and failure to balance between the exploration and exploitation phases. In order to address the previous shortcomings, we propose two-pronged enhancements: (1) the injection of fuzzy mutation; and (2) adding a decreasing time-dependent factor to achieve the exploration–exploitation balance.

4.1 The injection of Fuzzy mutation

Fuzzy logic describes the fuzziness as Membership Functions (MFs) in a graphical form that is used in fuzzy set theory. The issues discussed above are addressed by improving CapSA using a fuzzy mutation called centroid-based fuzzy mutation. This mutation prevents premature convergence of search agents. A mutation is applied depending on its probability. The probability of mutation (P_i) is given by,

Table 5 The mean, and STD of fitness values for 30 runs obtained by the competitor algorithms on the CEC'2020 functions with dim = 10

F#	Measure	mCapSA	CapSA	PSO	CMA-ES	GSA	WOA	HHO	AOA
1	Mean	57,774.59	1.33E+09	2722.599	1473.465	4,120,692	56,765,151	87,682.51	**287.6046**
	SD	75,230.11	4.36E+08	2454.018	1795.03	1,110,951	1.06E+08	135,332.9	257.5508
2	Mean	**2278.862**	4157.067	2942.733	2849.29	3050.653	3779.455	5357.955	4135.203
	SD	376.8344	459.4572	530.7278	538.4246	463.3832	557.7885	829.1069	537.0174
3	Mean	**751.8138**	840.626	758.656	761.1005	905.724	926.9826	811.6151	777.1336
	SD	10.47052	16.20023	13.17541	11.12685	24.18412	47.27067	8.240215	15.95857
4	Mean	**1904.546**	1923.502	**1904.466**	**1904.332**	1923.863	1956.317	**1904.627**	1967.138
	SD	3.443114	12.82267	0.890588	1.524792	6.326033	51.159	1.404748	40.14008
5	Mean	158,514.3	2,456,668	**128,493.6**	95,661.38	478,455.4	1,459,383	1,308,017	802,157.8
	SD	113,842.5	2,889,351	81,392.91	54,372.67	333,189.4	1,330,645	1,056,412	291,812.5
6	Mean	1948.126	1746.048	1976.921	**1726.992**	2234.764	2438.385	2117.649	2867.152
	SD	172.1316	87.69753	131.5999	85.68643	248.604	261.5383	170.2656	210.0235
7	Mean	**81,880.03**	764,786.6	84,396.97	103,120.9	178,473	1,235,867	548,235	485,391.1
	SD	44,691.67	724,344.2	71,383.56	59,885.75	144,702.9	1,169,516	416,453.9	207,733.2
8	Mean	**2302.73**	5036.113	3268.6	4271.042	3026.221	4110.059	6752.857	3484.568
	SD	1.283546	2036.938	1237.164	1920.907	1458.297	1867.125	868.34	1540.111
9	Mean	2865.025	2928.665	2867.691	2865.302	3121.373	2988.309	**2841.622**	3178.992
	SD	19.30359	20.42701	39.97781	22.49748	100.083	75.21588	42.37413	87.78172
10	Mean	2973.998	2971.261	2937.89	2993.499	2981.314	3041.337	**2906.27**	2993.027
	SD	30.0435	56.15338	30.01468	13.25813	35.97589	49.74076	0.006741	10.5448

The bold values are the best

$$P_i = \rho \times P_d + \varphi \times P_c \tag{48}$$

where $\rho = 0.6$ and $\varphi = 0.4$, P_d and P_c are given by,

$$P_d = \frac{1}{1 + \text{dist}} \tag{49}$$

$$P_c = a + b \times \tanh\left(\left(\frac{\text{unchanged}}{\alpha}\right) - \beta\right) \tag{50}$$

dist is the distance of the agent from the centroid, $a = 0.5$, $b = 0.5$, $\alpha = 4$, and $\beta = 5$, and unchanged is the number of iterations for which the global best agent has remained unchanged.

If the P_c is greater sufficient to achieve the agent mutation, the mutation occur is given by,

$$\triangle q = 0.5 \times (U - L) \times \left(1 - \frac{t}{T}\right)^2 \tag{51}$$

U and L are the bound of the problem, t current iteration, and T is the total number of iterations.

4.2 Exploration–exploitation balance

From exploration to exploration, the CapSA heavily relies on random parameters. As can be seen, the CapSA searches through a large number of random values without avoiding the immobility of local optimal solutions. So, here it will be replaced with the decreasing time dependent factor that is given by,

$$d^{t+1} = \exp\left(1 - \frac{(t - T)}{T}\right) \tag{52}$$

d^{t+1} decreases with time to decrease the randomization with time; therefore, the operation transfers from global part to local part with dynamic behavior. However, the pseudocode of the prepared mCapSA is illustrated by the following Algorithm 1.

In conclusion, the proposed mCapSA has successfully overcome the original CapSA limitations, avoiding local optimum, more balance between exploration and exploitation by introducing decreasing time-dependent factor given by Eq. (52). Moreover, mCapSA has many other advantages such as the injection of Fuzzy mutation in the original CapSA given by Eqs. (48, 49, 50 and 51).

5 Performance estimation of mCapSA

The CEC'2020 test suite is implemented for evaluating the performance of the developed mCapSA against quantitatively and qualitatively derived metrics. The statistical
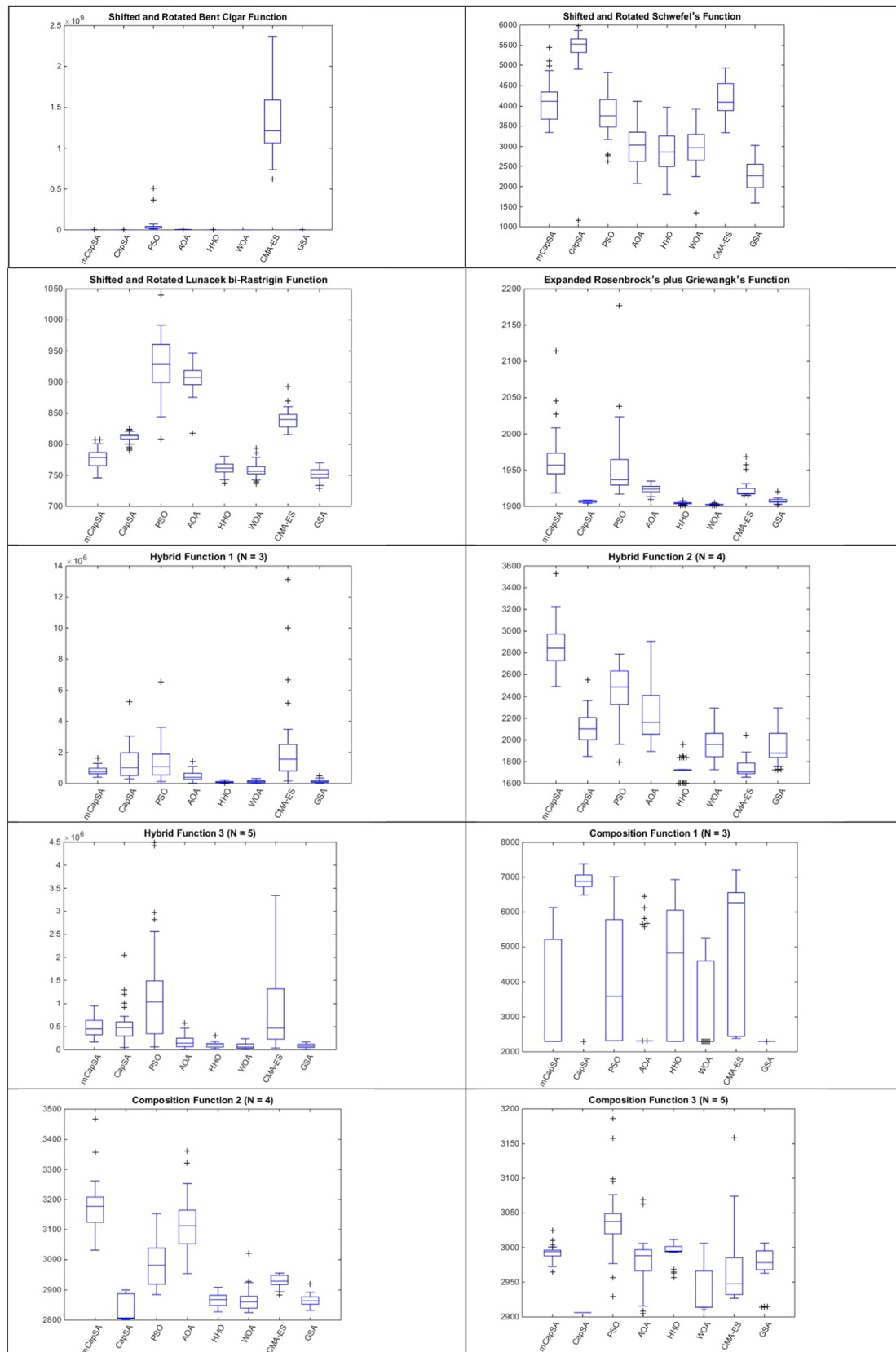
Fig. 3 The boxplot curves of the proposed mCapSA and the competitor algorithms obtained over CEC'2020 functions with Dim = 10

metrics such as the mean and standard deviation (STD) for best-practice outcomes are determined for the prepared mCapSA methodology and the corresponding item. Moreover, qualitative metrics considering boxplot and convergence curves are implemented. The proposed mCapSA outcomes have been compared with other 7 techniques namely, Particle swarm optimization (PSO) [48], Evolution strategy with covariance matrix adaptation (CMA-ES) [49], Gravitational search algorithm (GSA) [50], Whale optimization algorithm (WOA) [51], Harris' Hawks optimization (HHO) [52], Archimedes optimization algorithm (AOA) [53], and the original CapSA [47].

5.1 Parameters setting

It is noted in [57] that the parameters (that is, the population size) of the algorithms used affect the performance of the optimization algorithm and the quality of the search process. To achieve fair and statistically significant comparative benchmarking, in addition to considering that the algorithm's nature is stochastic, each algorithm used in the comparison process has its own parameters that must be set to their default values.

Algorithm 1: Pseudo code of the prepared mCapSA.

1. **Initialization Phase;**
2. Initialize parameters ($\epsilon 1$, $\epsilon 2$, N, T, P)
3. Initialize the population x_i (i = 1, 2, . . . N) randomly
4. Initialize the velocities v_i (i = 1, 2, . . . N) randomly
5. Evaluate initial solutions
6. Find the best solution and the global optimum;
7. select r random some leaders (<n/2)
8. While (t < T) do
9. Update τ using Eq. (40)
10. Update d^t using Eq. (52)
11. For each agent i, do
12.   Update agents' velocities using Eq. (41)
13.   if ($\epsilon 1 > 0.9$) then
14.   if ($d^t \leq 0.8$) then
15.   if ($\epsilon 2 \leq 0.01$) then
16.   Update leader's position that leap on the trees using Eq. (38)
17.   Else if ($\epsilon 2 \leq 0.99$) then
18.   Update leader's position that leap over riverbanks using Eq. (42)
19.   Else
20.   Update leader's position that walks on the ground using Eq. (43)
21.   End if
22.   Else if (P< $\epsilon 1 \leq 0.9$) then
23.   Update leader's position that swing on tree branches using Eq. (44)
24.   Else if ($\epsilon 1 > 0.95$) then
25.   Update leader's position that climbs on trees using Eq. (45)
26.   Else
27.   Update leader's position that relocates randomly using Eq. (46)
28.   End if
29.   Else
30.   Update leader's position of the followers using Eq. (47)
31.   End if
32. End for
33. Evaluate each solution
34. Sort and update P_c using Eq. (50)
35. if (P_c > th) then
36.   Update solution by applying mutation using Eq. (51)
37. Else
38.   No change
39. END IF
40. Check the ending situation. In the case of the ending criterion is fulfilled, the technique will be ended, or else return to Step 5
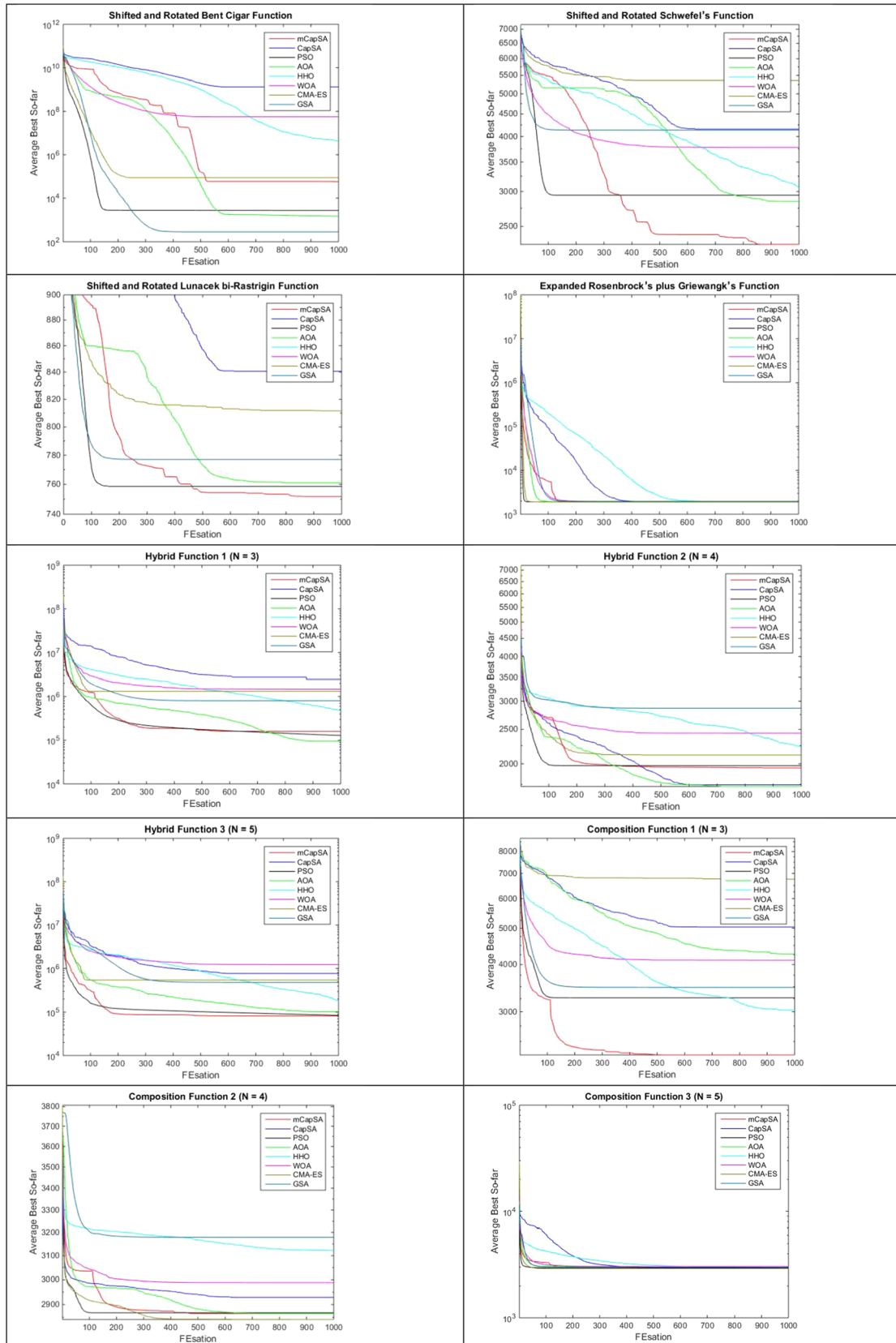
Fig. 4 The convergence curves of the proposed mCapSA and the competitor algorithms obtained on CEC'2020 functions with Dim = 10

For fair evaluation, the proposed mCapSA algorithm and the counterparts are evaluated in the same common setting. The initial parameter settings of these algorithms (default values) are reported in Table 4. For fair benchmarking comparison, the population size N was set to 30, the dimension of the optimization problem Dim was set as 10, each algorithm performs 30 runs for each function, the maximum number of function evaluations (FEs) are selected as 100,000.

5.2 Concept of CEC'2020 benchmark functions

Current subsection presents the estimation operation of the novel form of the CapSA named mCapSA. The IEEE Congress on Evolutionary Computation (CEC) [58] is then developed as test problems to evaluate the performance of the prepared techniques. First, the CEC'2020 benchmark functions contained 10 test functions, including multimodal, unimodal, hybrid, and composition functions, for more details see [59]. Figure 2 illustrates the 2D visualization of CEC'2020 functions, making the differences and nature of each issue easier to understand.

5.3 Statistical results

Table 5 presents the most significant results from the proposed mCapSA technique and the counted items for the statistical metrics over the CEC'2020 benchmark function with Dim = 10. The most promising results (lower values) are indicated in bold-red. The determined results revealed

Table 6 The Wilcoxon test results ($p \geq 0.05$) for each CEC'2020 function

F#	mCapSA versus CapSA	mCapSA versus PSO	mCapSA versus CMA–ES	mCapSA versus GSA	mCapSA versus WOA	mCapSA versus HHO	mCapSA versus AOA
1	3.02E−11	3.02E−11	3.02E−11	3.02E−11	3.02E−11	0.994102	3.02E−11
2	3.02E−11	1.39E−06	5.97E−05	1.25E−07	8.99E−11	5.57E−10	3.02E−11
3	3.02E−11	0.05012	0.002624	3.02E−11	3.02E−11	3.02E−11	5.53E−08
4	1.96E−10	5.07E−10	5.86E−06	1.33E−10	4.08E−11	0.446419	3.34E−11
5	1.78E−10	0.437641	0.026077	4.12E−06	1.41E−09	1.33E−10	4.98E−11
6	7.04E−07	0.549327	1.7E−08	8.29E−06	1.85E−08	0.000856	3.02E−11
7	5E−09	0.549327	0.245814	0.004856	8.1E−10	1.55E−09	3.34E−11
8	3.02E−11	0.520121	0.048413	3.02E−11	3.02E−11	5.57E−10	0.830253
9	9.92E−11	0.482517	0.876635	3.02E−11	1.61E−10	0.153667	3.02E−11
10	0.149449	6.28E−06	0.007959	0.641424	1.43E−08	2.99E−11	0.029205

Fig. 5 The single line diagram of 33-bus standard PDG
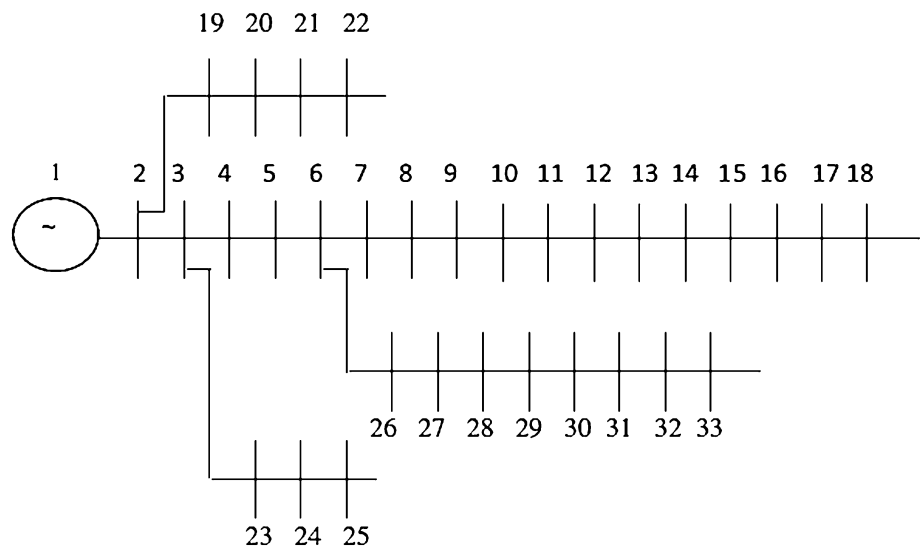
Table 7 The results of comprised proposed techniques on standard PDGs at different scales (33 and 118)

Order	Proposed method	Q_{DST} size (MVAr)/bus	$Q_{DST, Tot}$ (MVAr)	P_{Loss} (kW)	LR%	Q_{Loss} (kVAr)	V_{min} (p.u.)	VSI_{min} (p.u.)	Energy$_{Cost}$ ($)
Case 1: 33-bus standard PDG									
Base case		–	–	210.9678	–	143.013	0.9038	0.6672	2,115,286.523
6	AOA	0.5609/24 1.0109/30 0.4179/14	1.9897	138.3617	34.4157	94.3379	0.9347	0.7633	1,387,295.941
7	HHO	0.4993/24 1.0653/30 0.4212/14	1.9859	138.4371	34.3800	94.3968	0.9352	0.7649	1,388,051.669
4	WOA	0.5501/24 1.0506/30 0.4140/14	2.0147	138.3545	34.4191	94.3457	0.9348	0.7638	1,387,223.447
8	GSA	0.5653/24 1.0091/30 0.4223/14	1.9968	138.3896	34.4025	94.3616	0.9348	0.7638	1,387,575.665
5	CMA-ES	0.5500/24 1.0501/30 0.4150/14	2.0150	138.3591	34.4170	94.3492	0.9349	0.7639	1,387,269.551
3	PSO	0.5489/24 1.0536/30 0.4150/14	2.0175	138.3654	34.4139	94.3550	0.9349	0.7640	1,387,332.974
2	CapSA	0.5501/24 1.0525/30 0.4120/14	2.0146	138.3468	34.4228	94.3400	0.9347	0.7636	1,387,146.526
1 Best	**mCapSA**	**0.5400/24 1.0549/30 0.4086/14**	**2.0035**	**138.3305**	**34.4305**	**94.3241**	**0.9347**	**0.7632**	**1,386,982.639**
Case 2: 118-bus standard PDG									
Base case		–	–	1297.7	–	978.471	0.8688	0.5698	13,011,688.314
5	AOA	1.8355/101 1.4644/31 1.0056/42 2.2429/110 2.3342/50 1.7181/74 1.9349/80 1.0486/96	13.5842	832.3679	35.8591	619.149	0.9137	0.6970	8,345,808.270
7	HHO	2.3111/101 1.3214/31 0.8505/42 2.3105/110 2.2918/50 1.5717/74 1.7968/80 1.4841/96	13.9379	833.0772	35.8045	620.192	0.9119	0.6914	8,352,919.587

Table 7 (continued)

Order	Proposed method	Q_{DST} size (MVAr)/ bus	$Q_{\text{DST, Tot}}$ (MVAr)	P_{Loss} (kW)	LR%	Q_{Loss} (kVAr)	$V_{\min}$ (p.u.)	VSI$_{\min}$ (p.u.)	Energy$_{\text{Cost}}$ ($)
4	WOA	2.4444/101 1.9013/31 1.0195/42 2.2736/110 2.1919/50 1.6323/74 2.0088/80 1.2644/96	1.47361	832.3068	35.8638	620.764	0.9129	0.6944	8,345,196.046
8	GSA	2.0677/101 2.1307/31 1.2448/42 2.2593/110 2.1577/50 1.6491/74 1.8360/80 1.2495/96	14.5947	834.0682	35.7281	621.964	0.9128	0.6941	8,362,856.281
6	CMA-ES	2.0682/101 2.1579/31 1.1500/42 2.2603/110 2.1557/50 1.6477/74 1.8348/80 1.2472/96	14.5217	832.4310	35.8543	620.869	0.9127	0.6940	8,346,440.848
3	PSO	2.0559/101 0.8814/42 0.6947/23 2.2597/110 2.7025/50 1.6454/74 1.8306/80 1.2444/96	13.3146	832.2993	35.8644	619.909	0.9128	0.6941	8,345,120.367
2	CapSA	2.0306/101 2.5433/31 0.7714/42 2.1668/110 2.0872/50 1.5931/74 2.0283/80 1.2830/96	14.5036	830.6876	35.9886	620.845	0.9122	0.6924	8,328,960.071

Table 7 (continued)

Order	Proposed method	Q_{DST} size (MVAr)/bus	$Q_{DST,\ Tot}$ (MVAr)	P_{Loss} (kW)	LR%	Q_{Loss} (kVAr)	V_{min} (p.u.)	VSI_{min} (p.u.)	Energy$_{Cost}$ ($)
1 Best	**mCapSA**	**1.9700/31** **1.3368/104** **0.7874/42** **1.9451/110** **2.1802/50** **1.6421/74** **1.8622/80** **1.2762/96**	**13.0000**	**828.0562**	**36.1914**	**616.803**	**0.9128**	**0.6941**	**8,302,576.958**

Order	Proposed method	CAP$_t$ ($)	Saving (%)	ObjF$_1$	ObjF$_2$	ObjF$_3$	ObjF$_4$	MObjF	CPU speed (s)/FEs
Case 1: 33-bus standard PDG									
Base case		2,115,286.523	–	–	–	–	–	–	0.9525 (s)/Non
6	AOA	1,455,767.806	31.1787	0.6558	0.6036	0.3247	0.5923	0.571426	122.767 (s)/200
7	HHO	1,456,402.426	31.1487	0.6562	0.6059	0.3198	0.5922	0.571308	127.050 (s)/200
4	WOA	1,456,496.264	31.1442	0.6558	0.6050	0.3217	0.5922	0.571248	121.093 (s)/200
8	GSA	1,456,276.124	31.1546	0.6559	0.6040	0.3239	0.5923	0.571443	120.735 (s)/200
5	CMA-ES	1,456,551.698	31.1416	0.6558	0.6051	0.3216	0.5922	0.571250	123.496 (s)/200
3	PSO	1,456,697.403	31.1347	0.6558	0.6052	0.3213	0.5921	0.571245	126.776 (s)/200
2	CapSA	1,456,415.847	31.1481	0.6557	0.6049	0.3219	0.5922	0.571243	119.559 (s)/200
1 Best	**mCapSA**	**1,455,899.207**	**31.1725**	**0.6556**	**0.6046**	**0.3225**	**0.5923**	**0.571240**	**108.878 (s)/200**
Case 2: 118-bus standard PDG									
Base case		13,011,688.314	–	–	–	–	–	–	0.9651 (s)/Non
5	AOA	8,793,315.527	32.4199	0.6414	0.5967	0.3000	0.5967	0.558286	247.0665 (s)/200
7	HHO	8,811,745.127	32.2782	0.6420	0.5963	0.3006	0.5962	0.558477	241.8300 (s)/200
4	WOA	8,829,565.230	32.1413	0.6414	0.5985	0.2952	0.5957	0.557787	273.4037 (s)/200
8	GSA	8,842,701.093	32.0403	0.6427	0.5984	0.2960	0.5954	0.558484	232.8189 (s)/200
6	CMA-ES	8,823,950.872	32.1844	0.6415	0.5981	0.2966	0.5959	0.557990	248.3261 (s)/200
3	PSO	8,784,002.038	32.4915	0.6414	0.5967	0.2995	0.5970	0.558152	244.8752 (s)/200
2	CapSA	8,805,888.994	32.3232	0.6401	0.5974	0.2984	0.5964	0.557556	237.2244 (s)/200
1 Best	**mCapSA**	**8,731,388.804**	**32.8958**	**0.6381**	**0.5968**	**0.2998**	**0.5984**	**0.556862**	**230.4002 (s)/200**

Bold items represent the numerical results based on mCapSA technique

the superiority of the proposed mCapSA algorithm compared to its counterparts in solving six of functions from the CEC'2020 test suite. Moreover, the first rank in terms of mean and STD is recorded for the developed mCapSA methodology.

5.4 Boxplot performance analysis

Figure 3 displays boxplot curves for the proposed mCapSA method and corresponding items to depict data distributions into quartiles over the ten CEC'2020 test suite for Dim = 10. The lowermost and largest data items reached by the algorithms are presented as the minimum and maximum values in the boxplot's curves, which are the edges of the whiskers. The lower and upper quartiles are restricted by the ends of the rectangles. A narrow boxplot indicates that the data are closely matched. For most functions, the boxplot analysis demonstrated that the proposed mCapSA technique realized the most suitable distribution with the lowest values in comparison with the other challenger algorithms.

5.5 Convergence performance analysis

The convergence-curves of the proposed mCapSA method and the counterparts over the 10 of CEC'2020 test suite for Dim = 10 are provided by Fig. 4. It is noteworthy that the developed mCapSA algorithm obtained the lowest values

Table 8 The existing values of SIA method based on SIL via VSI for 33-bus standard PDG

Bus Nº	SIL	VSI
6	**0.01448**	**0.8011**
28	**0.01203**	**0.7332**
29	**0.00899**	**0.7219**
8	**0.00727**	**0.7354**
3	**0.00675**	**0.9064**
7	**0.00440**	**0.7560**
5	**0.00390**	**0.8140**
4	**0.00389**	**0.8790**
24	*0.00374*	*0.8828*
13	**0.00356**	**0.6835**
9	**0.00334**	**0.7168**
10	**0.00316**	**0.7140**
30	*0.00308*	*0.7090*
31	**0.00300**	**0.7061**
27	**0.00187**	**0.7598**
25	**0.00186**	**0.8063**
14	*0.00183*	*0.6792*
23	**0.00181**	**0.8949**
17	**0.00158**	**0.6672**
26	0.00137	0.7977
2	0.00136	0.9354
32	0.00075	0.7053
15	0.00072	0.6751
16	0.00066	0.6690
22	0.00048	0.9198
12	0.00044	0.6904
11	0.00026	0.7093

Bold items shows the 2/3 of the existing results by SIL based VSI methodology. The italic highlights illustrates the optimum location of DSTATCOM by mCapSA technique

of the ObjF for most functions, meaning that the prepared technique is capable of achieving convergence quickly. Furthermore, this convergence can be observed, making the proposed mCapSA a promising optimization tool for solving online optimization problems which require fast calculations.

5.6 Statistical analysis using Wilcoxon's rank sum test

As a means of assessing the significance of the results and complementing the statistical analysis, Wilcoxon rank sum tests can be performed. A Wilcoxon test is carried out to ensure that the evaluated performance is relatively stable and not random. In [59], the Wilcoxon rank sum test is described in detail. Using paired methods, Table 6

presents a comprehensive analysis of the average of the highest quality solutions to date. This test has a significance level of 5%. Based on the fact that the p-values for most functions are ≤ 0.05 (5% significance level), the results for the four classes of the CEC'2020 test suite are statistically significant. This confirms that the performance of the mCapSA algorithm is not random. In conclusion, the optimum solutions are achieved by applying an applicable and prearranged set of optimization rules.

6 The existing results

The suggested scheme utilizing the mCapSA technique was executed by means of MATLAB package'R2021a that is executed on an Intel® Core^{TM} i5-5200U CPU @2.20 GHz including a memory of 6.00 GB and 64-bit operational system. Based on the above methodology steps considering the AHP algorithm, the optimal weights κ_1, κ_2, κ_3, and κ_4 for the MObjF are concluded as 0.4498, 0.2950, 0.1973, and 0.0579, respectively. Moreover, the λ_{max} = 4.1155, while, the consistency and index ratios, respectively, are $I_{CR} = 0.0428$ and $I_{CI} = 0.0385$, respectively. Supplementary, the reciprocal matrix [A] can be deduced as follows,

$$A = \begin{bmatrix} 1 & 1 & 3 & 9 \\ 1/1 & 1 & 1 & 5 \\ 1/3 & 1/1 & 1 & 3 \\ 1/9 & 1/5 & 1/3 & 1 \end{bmatrix}$$

The results of this work are performed considering 4 cases. In the first and second cases, the proposed scheme was applied to 33-bus and 118-bus PDGs to assess the performance of the studied optimization techniques with the modified mCapSA method. Based on the comprehensive analysis with recently published optimizers for DSTATCOM allocation, the mCapSA was validated. Ultimately, the DSTATCOM performance based on the mCapSA method was evaluated using the Egyptian case study as a real load model applied to a 33-bus PDG for 24 h.

6.1 Case1: The results of 33-bus standard power distribution grid (PDG)

The prepared methodology is tested on 33-bus standard PDG, where the rated line voltage and MVA are 12.66 kV and 100 MVA, respectively. The data of the 33-bus model is given by [60]. Figure 5 illustrates the 33-bus single line diagram. As illustrated in Table 7, in the base case, the total active (P_{loss}) and reactive (Q_{loss}) power losses are 210.9678 kW and 143.013 kVAR, respectively. Moreover, the minimum voltage profile (V_{min}) is 0.9038 p.u, minimum
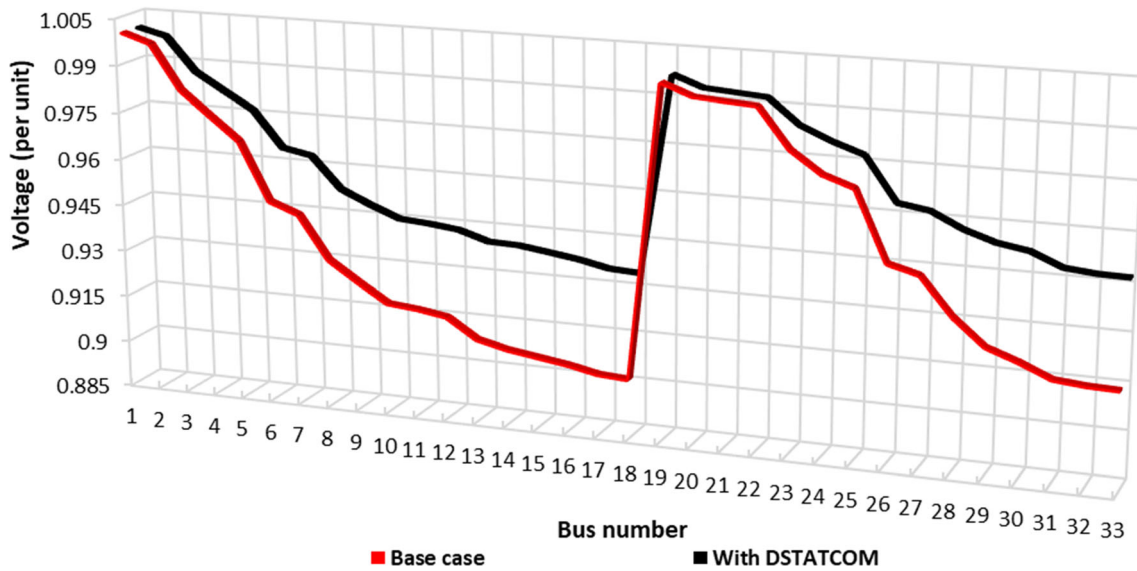
Fig. 6 The result of compensated devices on voltage levels for 33-bus standard PDG
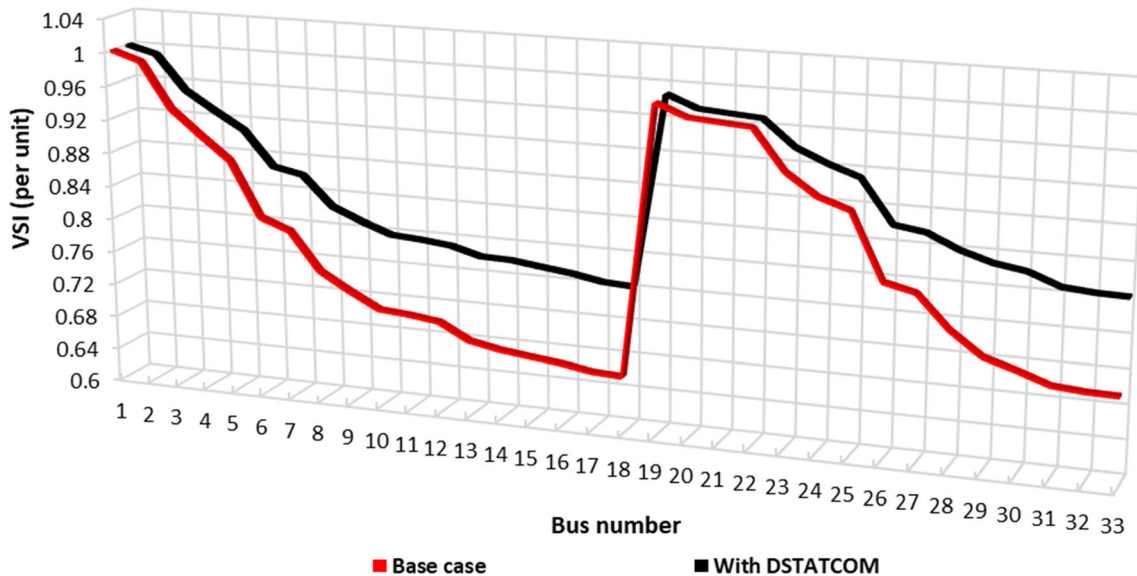

Fig. 7 The influence of compensated devices on voltage stability for 33-bus standard PDG

voltage stability index (VSI$_{min}$) is 0.6672 p.u, and the capital annual price (CAP$_t$) is 2,115,286.523 \$. However, the existing results of the SIA algorithm based on the SIL and VSI methodology are shown in Table 8. The proposed mCapSA technique elected the optimal nodes 24, 30, and 14 for DSTATCOM location from 2/3 of the SIL results.

mCapSA and the other recently proposed optimizers have been compared for allocating DSTATCOM in the most appropriate positions and sizes (MVAr) as shown in Table 7, where the optimal locations are 24(0.540), 30(1.0549), and 14(0.4086). Based on the comprehensive analysis performed, it is quite evident that mCapSA is superior in finding optimal solutions to the proposed problem, where the active power loss reduction (LR) is minimized by 34.4305% and the capital annual price (CAP$_t$) is saved by 31.1725%. The AOA method has the highest net saving of 31.1787%, but it has the lowest LR of 34.4157% when compared with mCapSA. Moreover, all the proposed methods such as original CapSA, PSO, WOA, CMA-ES, AOA, HHO, and GSA have higher values of V_{min} and VSI$_{min}$ compared to mCapSA. However, mCapSA has the lowest values of active (138.3305 kW) and reactive (94.3241 kVAr) power losses, and its performance spent only 108.878 s in 200 function evaluations,
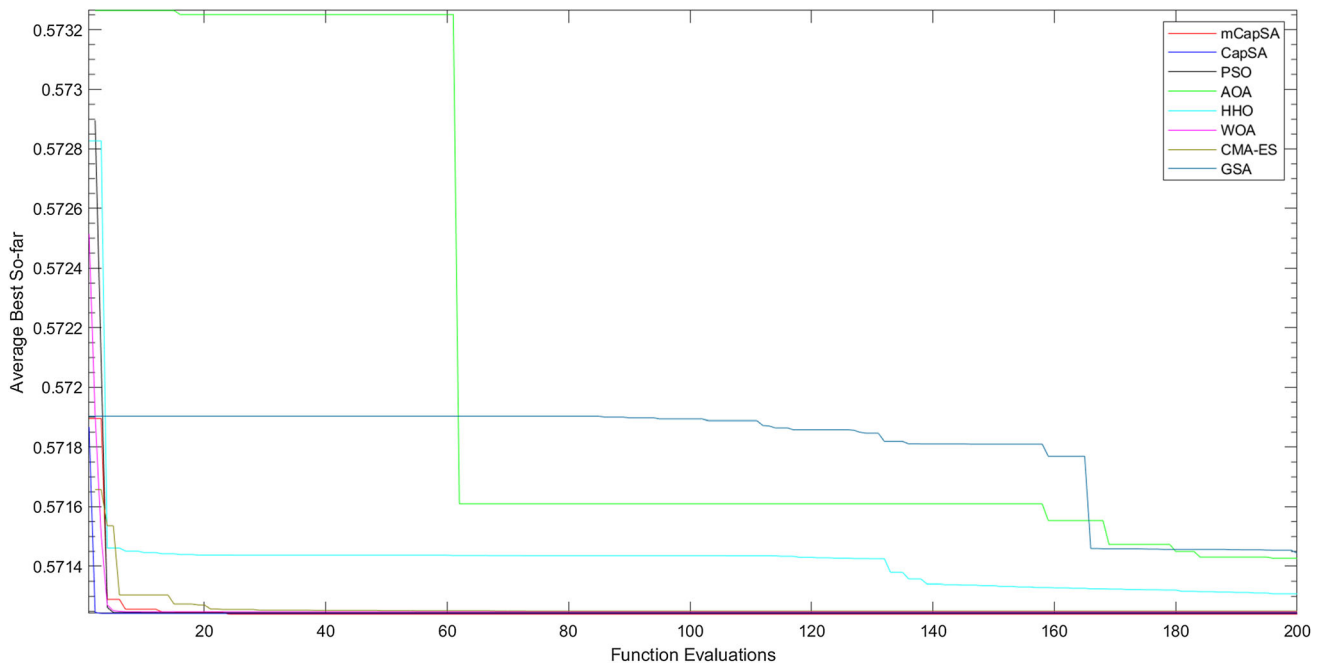
Fig. 8 The performance of the objective function via function evaluations for 33-bus standard PDG
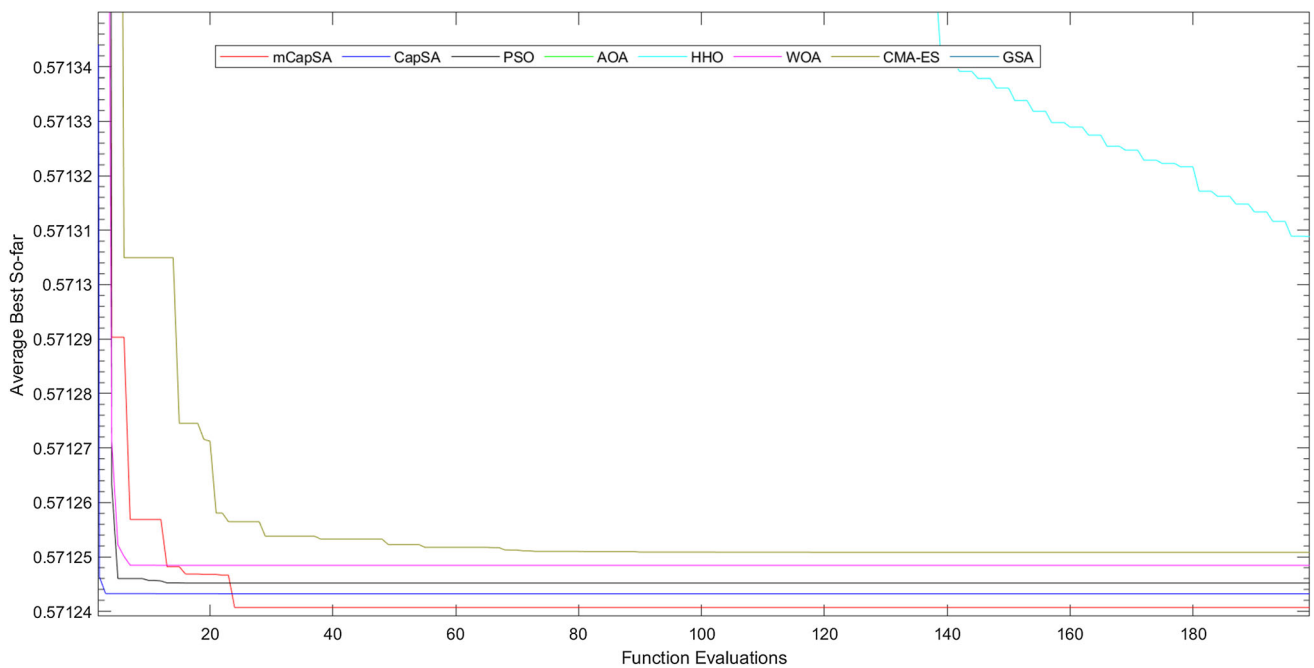
Fig. 9 The zoom-in of the performance of the objective function via function evaluations for 33-bus standard PDG

the shortest CPU time. Furthermore, the mCapSA has the lowest energy costs (1,386,982.639 \$) and CAP_t (1,455,899.207 \$), except the AOA method.

Figures 6 and 7 explain the performance effect of the DSTATCOM devices on the voltage and stability profiles.

In addition, the convergence of the *MObjF* with the function evaluations has been illustrated in Fig. 8. Moreover, Fig. 9 zooms in from Fig. 8 that illustrates the superiority in convergence of the mCapSA algorithm to deduce the optimal MObjF value of 0.571240.
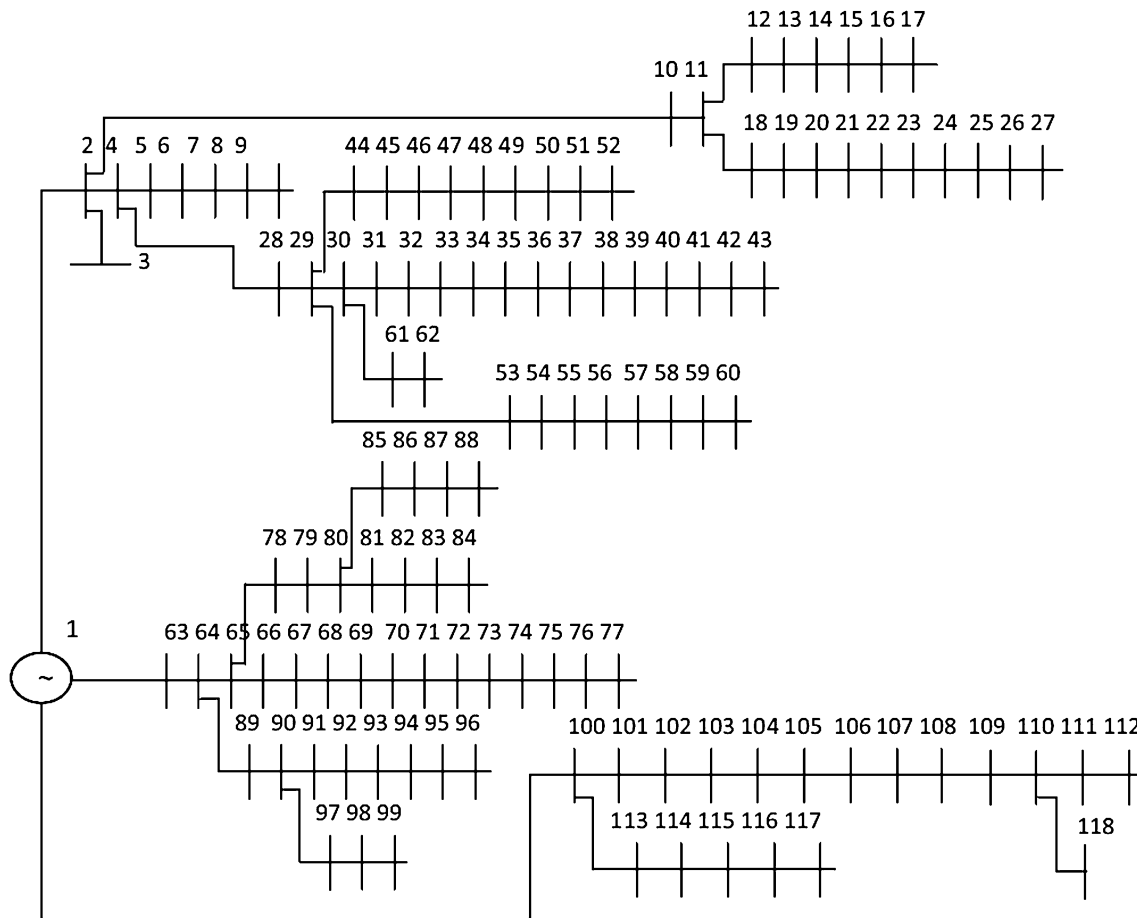
Fig. 10 The single line diagram of 118-bus standard PDG

6.2 Case2: The results of 118-bus standard power distribution grid (PDG)

The 118-bus standard PDG is displayed in Fig. 10. The 118-bus PDG rated line voltage is 11 kV and the rated MVA is 100. The PDG data in details can be found at [61]. According to Table 7, the base case of 118-bus PDG illustrates that the P_{loss} and Q_{loss} are 1297.7 kW and 978.471 kVAr, respectively, the V_{min} is 0.8688 pu, VSI_{min} is 0.5698 pu, the CAP_t is 13,011,688.314 \$.

In Table 9, the deduced results of the SIA method are used to reduce the research space needed by the developed optimizers. This is done to determine the most critical location for DSTATCOM devices. Thus, the proposed optimizers have been optimized (2/3) using the existing results of the SIA method. From Table 7, the optimizers were elected based on the most optimum locations in the following nodes {101, 31, 104, 42, 23, 110, 50, 74, 80, 96}. The existing result in Table 7 proved that the superiority of the proposed mCapSa to deduce the optimal solutions relative that has the highest LR = 36.1914% and the CAP net savings = 32.8958%, in addition, it has the lowest

capacity of the total DSTATCOM value = 13.0000 MVAr. As illustrated by Table 7, despite the AOA and WOA having the highest values of V_{min} and VSI_{min}, they failed to find the global optimum of the other parameters. Figures 11 and 12 represented the influence of the DSTATCOM allocation on the voltage and stability index profiles. Figure 13 shows how the MObjF compares with functional evaluations, where the value of 0.556862 pu is the lowest among the optimization algorithms, while the mCapSA optimizer can complete its task in 230.4002 s. According to these results, the mCapSA has strong ability to obtain optimal solutions at different scales of the distribution grids.

6.3 Case3: The comprehensive analysis with the last studies from literature

In case 3, a comprehensive analysis has been conducted between the proposed modified CapSA algorithm, its original case, and the most recent published optimizers. This analysis has been conducted to ensure the validity and ability of the proposed mCapSA to achieve the global

Table 9 The existing values of SIL via VSI algorithm for 118-bus standard PDG

Bus Nº	SIL	VSI	Bus Nº	SIL	VSI	Bus Nº	SIL	VSI	Bus Nº	SIL	VSI
70	**0.024808**	**0.6108**	*110*	*0.003658*	*0.6717*	**41**	**0.001793**	**0.8408**	60	0.000402	0.8798
30	**0.018157**	**0.8527**	**39**	**0.003574**	**0.8913**	**100**	**0.001745**	**0.9363**	14	0.000397	0.9466
64	**0.016101**	**0.8791**	**63**	**0.003558**	**0.9277**	**56**	**0.001711**	**0.9107**	112	0.000388	0.6770
101	*0.014096*	*0.9083*	**40**	**0.003466**	**0.8787**	**55**	**0.001705**	**0.9224**	25	0.000367	0.8723
31	*0.012935*	*0.8366*	**49**	**0.003445**	**0.7068**	**51**	**0.001646**	**0.6968**	75	0.000362	0.5701
78	**0.010817**	**0.8508**	*50*	*0.003361*	*0.6995*	**111**	**0.001593**	**0.6774**	93	0.000324	0.8015
68	**0.010165**	**0.7198**	**36**	**0.003167**	**0.8840**	**57**	**0.001499**	**0.8879**	61	0.000182	0.8780
33	**0.009460**	**0.7806**	**79**	**0.003144**	**0.8404**	**71**	**0.001471**	**0.5976**	44	0.000163	0.8348
34	**0.009022**	**0.7615**	**19**	**0.003125**	**0.9134**	**97**	**0.001370**	**0.7909**	94	0.000162	0.8008
104	*0.007528*	*0.7952*	**20**	**0.003066**	**0.9075**	**81**	**0.001359**	**0.8290**	16	0.000158	0.9456
42	*0.006117*	*0.8372*	**48**	**0.002809**	**0.7187**	**12**	**0.001272**	**0.9492**	95	0.000154	0.7969
35	**0.006068**	**0.8868**	**29**	**0.002642**	**0.8992**	**82**	**0.000959**	**0.8269**	87	0.000134	0.8460
103	**0.005805**	**0.8153**	**105**	**0.002639**	**0.7605**	**86**	**0.000947**	**0.8463**	26	0.000117	0.8720
58	**0.005143**	**0.8844**	**32**	**0.002590**	**0.8076**	**53**	**0.000939**	**0.6842**	45	0.000116	0.8344
47	**0.005000**	**0.7313**	*74*	*0.002546*	*0.5747*	**54**	**0.000826**	**0.9360**	84	0.000105	0.8258
108	**0.004982**	**0.7006**	**66**	**0.002500**	**0.8145**	24	0.000702	0.8727	98	0.000095	0.7905
102	**0.004889**	**0.8716**	**107**	**0.002442**	**0.7125**	43	0.000700	0.8358	88	0.000083	0.8373
18	**0.004843**	**0.9254**	*80*	*0.002163*	*0.8327*	76	0.000651	0.5698	17	0.000073	0.9367
65	**0.004769**	**0.8530**	**90**	**0.002150**	**0.8068**	52	0.000594	0.6902	85	0.000071	0.8469
69	**0.004538**	**0.6203**	**72**	**0.002146**	**0.5858**	13	0.000567	0.9471	46	0.000067	0.7420
106	**0.004420**	**0.7440**	*96*	*0.002114*	*0.7914*	37	0.000560	0.9255	15	0.000062	0.9459
89	**0.004374**	**0.8217**	**91**	**0.002091**	**0.8039**	22	0.000533	0.8783	77	0.000045	0.8672
23	*0.004263*	*0.8740*	**109**	**0.001982**	**0.6799**	92	0.000508	0.8022			
67	**0.004164**	**0.7580**	**73**	**0.001969**	**0.5768**	59	0.000438	0.8811			
38	**0.003716**	**0.9037**	**21**	**0.001814**	**0.9045**	83	0.000404	0.8262			

Bold items shows the 2/3 of the existing results by SIL based VSI methodology. The italic highlights illustrates the optimum location of DSTATCOM by mCapSA technique
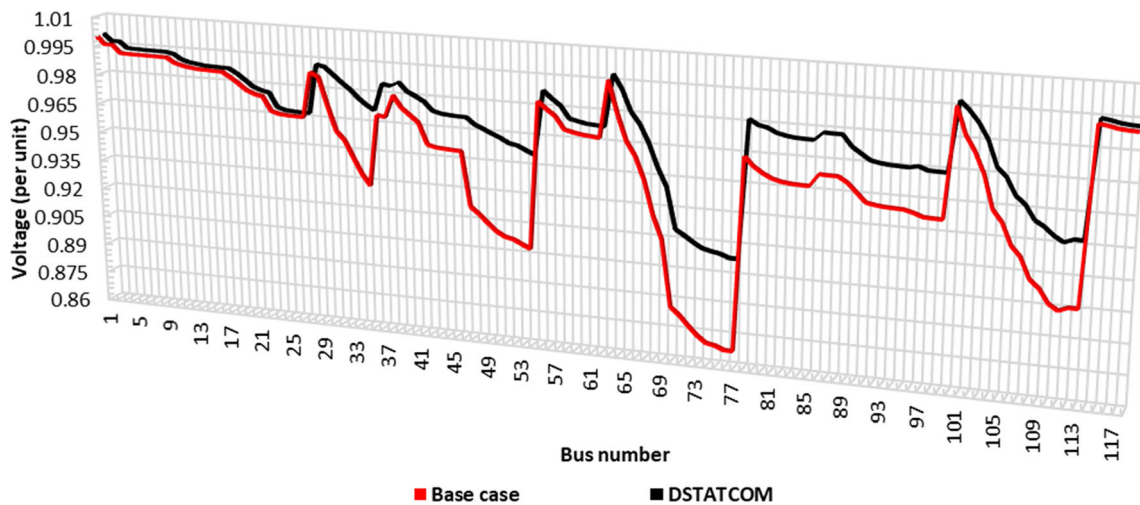

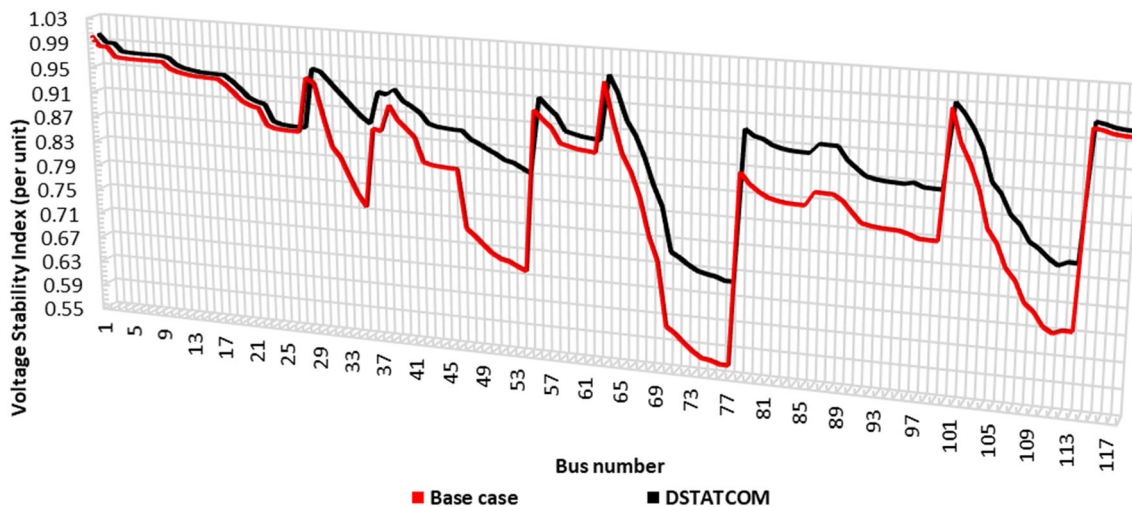**Fig. 11** The influence of DSTATCOM devices on voltage levels for 118-bus standard PDG

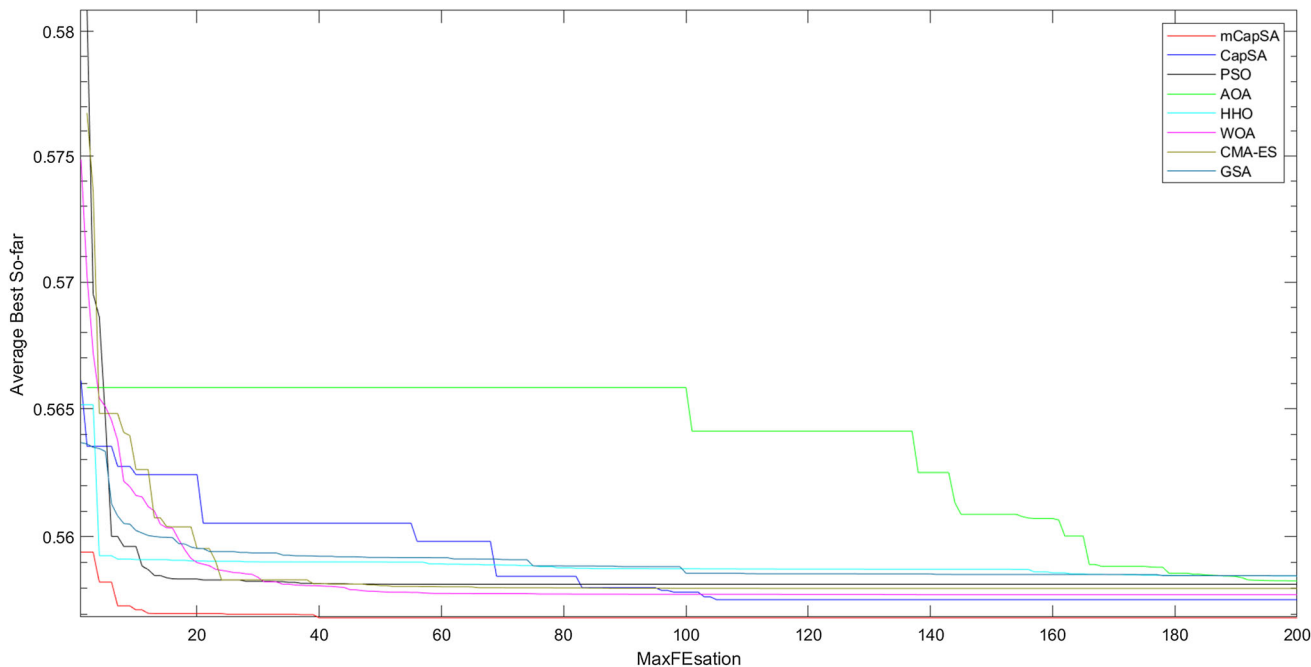**Fig. 12** The result of DSTATCOM devices on voltage stability for 118-bus standard PDG

Fig. 13 The performance of the objective function via function evaluations for 118-bus standard PDG

optimum of the current problem. However, Table 10 summarized the comprehensive study in two scenarios: 33-bus and 118-bus distribution systems.

The mCapSA was compared, in the case of 33-bus PDG, with its original one, as well as with PSO, FA, hybrid FA-PSO, FA-AAC-PSO, FA-APG-PSO, FA-TVA-PSO, FA-NDAC-PSO, and FA-SCAC-PSO [45]. Following Table 10, the optimization methods had been ordered to start with the highest optimum solutions based on mCapSA. By contrast, the mCapSA technique can reduce the power system losses by 34.4305%. In addition, it can

reduce the total energy cost by 1,386,982.639 $ as compared to previous optimization methods, including the original. Furthermore, the mCapSA can improve the minimum voltage level to 0.9347 p.u., the highest in this comprehensive study.

For the second case with 118-bus PDG, the mCapSA method was compared with its original one as well as with BFO [28], MOPSO [42], MOGROM [42], MOIGROM [42], and the original CapSA methods. In Table 10, the compared optimizers were sorted from the most optimum, which is mCapSA, to the least optimum, which is BFO.

Table 10 The comprehensive analysis between the proposed mCapSA and other methods in literature on 33-bus and 118-bus standard PDG

Technique	Q_{DST} size MVAr (bus)	P_{Loss}	LR %	Energy cost ($)	V_{min}	VSI_{min}	Algorithm order
Case 1: 33-bus distribution system							
Base case	–	210.9678	–	2,115,286.523	0.9038	0.6672	–
PSO [45]	0.3140 (15)	141.8247	32.7742	1,391,940.903	0.9324	–	10
	0.6569 (23)						
	1.1390 (29)						
FA [45]	0.4037 (14)	138.4071	34.3942	1,387,753.791	0.9345	–	5
	0.5668 (24)						
	1.0584 (30)						
FA-PSO [45]	0.4870 (11)	138.4244	34.3860	1,387,927.252	0.9312	–	8
	0.5629 (24)						
	1.0007 (30)						
FA-AAC-PSO [45]	0.4016 (14)	138.3928	34.4001	1,387,610.411	0.9344	–	4
	0.5298 (24)						
	1.0628 (30)						
FA-APG-PSO [45]	0.4126 (14)	138.4411	34.3781	1,388,094.696	0.9348	–	9
	0.5537 (24)						
	1.0572 (30)						
FA-TVA-PSO [45]	0.3982 (14)	138.4090	34.3933	1,387,772.842	0.9342	–	7
	0.6039 (24)						
	1.0464 (30)						
FA-NDAC-PSO [45]	0.4061 (14)	138.4074	34.3940	1,387,756.799	0.9346	–	6
	0.5524 (24)						
	1.0577 (30)						
FA-SCAC-PSO [45]	0.4021 (14)	138.3928	34.4001	1,387,610.411	0.9344	–	3
	0.5531 (24)						
	1.0594 (30)						
Proposed CapSA	0.5501 (24)	138.3468	34.4228	1,387,149.187	0.9347	0.7636	2
	1.0525 (30)						
	0.4120 (14)						
Proposed mCapSa	**0.5400 (24)**	**138.3305**	**34.4305**	**1,386,982.639**	**0.9347**	**0.7632**	**1 Best**
	1.0549 (30)						
	0.4086 (14)						
Case 2: 118-bus distribution system							
Base case	–	1297.7	–	13,011,688.314	0.8688	0.5698	–
BFO [28]	2.541 (38)	871.40	32.8504	8,737,186.560	0.9062	–	6
	1.425 (46)						
	1.521 (74)						
	1.715 (91)						
	2.021 (118)						
MOPSO [42]	1.371 (23)	851.54	34.3808	8,538,058.117	0.9272	–	4
	1.012 (31)						
	0.668 (46)						
	0.634 (64)						
	1.500 (68)						
	1.333 (70)						
	1.134 (78)						
	1.327 (103)						
	1.476 (108)						

Table 10 (continued)

Technique	Q_{DST} size MVAr (bus)	P_{Loss}	LR %	Energy cost ($)	V_{min}	VSI_{min}	Algorithm order
MOGROM [42]	0.295 (23)	852.20	34.3300	8,544,675.678	0.9271	–	5
	0.413 (30)						
	1.338 (42)						
	0.764 (58)						
	1.288 (78)						
	1.252 (104)						
	1.134 (78)						
	1.493 (106)						
	1.285 (108)						
	1.500 (113)						
MOIGROM [42]	1.494 (23)	850.73	34.4432	8,529,936.564	0.9273	–	3
	1.258 (47)						
	1.304 (64)						
	1.500 (70)						
	1.435 (78)						
	1.346 (89)						
	1.500 (101)						
	1.396 (106)						
Proposed CapSA	2.0306 (101)	830.6876	35.9886	8,328,960.071	0.9122	0.6924	2
	2.5433 (31)						
	0.7714 (42)						
	2.1668 (110)						
	2.0872 (50)						
	1.5931 (74)						
	2.0283 (80)						
	1.2830 (96)						
Proposed mCapSA	**1.9700 (31)**	**828.0562**	**36.1914**	**8,302,576.958**	**0.9128**	**0.6941**	**1 Best**
	1.3368 (104)						
	0.7874 (42)						
	1.9451 (110)						
	2.1802 (50)						
	1.6421 (74)						
	1.8622 (80)						
	1.2762 (96)						

Bold items indicate the best results by the proposed mCapSA

Although, the MOPSO, MOGROM, and MOIGROM have the highest minimum voltage level, the mCapSA methodology has the lowest energy cost (8,302,576.958 $) and the highest power system loss reduction (LR = 36.1914%).

According to the comprehensive analysis that is illustrated by Table 10, the mCapSA technique can find the optimal solution of the proposed scheme successfully. However, in this work, it is very relevant to examine the performance of the DSTATCOM with load levels that can be explained by the fourth case of the existing results.

6.4 Case 4: DSTATCOM performance study at different load levels of Egyptian case study

In the current case study, the performance of DSTATCOM has been studied considering load modeling based on the

Fig. 14 The utilized power analyzer (model HIOKI-3196 with the program of HIOKI-9624-50 "PQA-Hiview PRO")

practical measurement and analysis of the Middle Egyptian power distribution grid (MEPDG). As depicted in Fig. 14, a power analyzer has been applied for 24 h to different load points of the MEPDG. This is done to deduce the power quality of the measured system and to determine the power demand curve. The real load demand model illustrated by Fig. 15 is applied to 33-bus standard PDG in this study. It can be seen that the nominal load demand amounts to 84% of the load at 10:00 a.m. and 22:00 p.m., as illustrated in Fig. 15.

In the base case, the bus voltage and the voltage stability profiles are shown in Figs. 16a and 17a, respectively.

After installing the DSTATCOMs optimally at buses 14, 24, and 30 as illustrated by Fig. 18, the bus voltage and stability voltage profiles are improved to the extent shown in Figs. 16b and 17b, respectively. It has been illustrated by Fig. 18 that the DSTATCOMs devices compensate different reactive power at nodes 24 and 30 at all times with different load demand levels. The DSTATCOM device located at bus 14 absorbs reactive power from the grid with light loads from 01:00 a.m. to 8:00 a.m. and compensates reactive power from 9:00 a.m. to 00:00. These devices had a decisive impact on the performance of the grid using the mCapSA technique. The MCapSA successfully minimized the active and reactive losses as well as the installation and operating costs of installed devices. This is done while maximizing the net savings of the total annual price for the device and its energy consumption, as depicted in Figs. 19, 20, and 21, respectively.

However, Table 11 illustrates the values of active and reactive power losses that were reduced to 2926.5481 kW by 33.4673% of active loss reduction and to 2000.489 kVAr by 32.9098% of reactive loss reduction. Moreover, the total energy costs have been minimized to 1,222,636.99 $ with a net saving of 615,012.06 $. In addition, the total capital annual cost has been minimized to 1,284,197.56 $ with a net saving of 553,451.49 $.

To conclude, the mCapSA technique proved superior in finding the optimal allocation of DSTATCOM devices within the PDG, regardless of the load level.

Fig. 15 The spectrum of the real measured load curve in the MEPDG

Fig. 16 The voltage profile (per unit) at **a** the base case and **b** the case with mCapSA optimizer of 33-bus PDG at 24 (h)


(a)

(b)
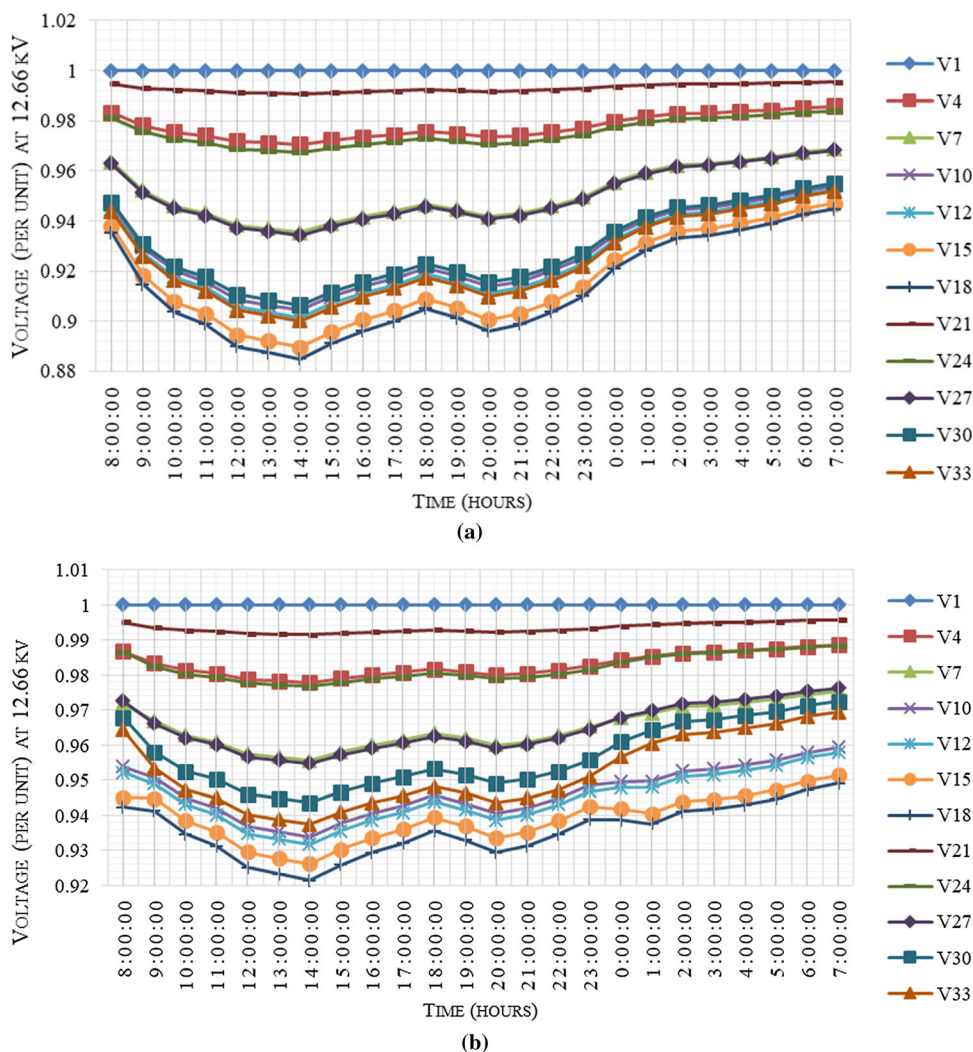
7 Conclusion

The prepared article presents an approach based on the modified Capuchin Search Algorithm (mCapSA) with sensitivity index algorithm (SIA) to deduce the optimum siting and capacity of DSTATCOM devices in the power distribution grids (PDGs). In order to estimate the power flow, the backward/forward sweep algorithm (BFS) was used. Moreover, the SIA has been employed to determine the farthest applicant nodes, which are required to minimize the search space for the proposed optimizer. By using the SIA method, the prepared mCapSA enables DSTAT-COM to determine the optimum capacity and siting of their existing buses. A multi-objective function (MObjF) approach is designed to improve the performance of the proposed system and provide global optimal solutions. The overall scheme has been verified on the 33-bus and 118-bus PDGs. To evaluate the DSTATCOM devices in practice,

the proposed scheme has also been applied to the 33-bus distribution system using the real load demand analysis of the middle Egyptian distribution grid (MEPDG). This case study demonstrates that the total net savings of capital annual price (CAP_t) is 30.1173% for 30 years, while the active and reactive loss reduction of the modeled distribution system are 33.4673% and 32.9098%, respectively, for 30 years. To investigate the performance of the prepared methodology, a comprehensive analysis of the existing results in conjunction with the newly and previously published techniques has been conducted. However, the proposed mCapSA technique proved superior in deriving the optimum allocation of the DSTATCOM devices in the PDGs. This was to enhance voltage levels, minimize system losses, and minimize CAP_t of the PDGs. A future work will conclude with the operation management of the distribution grids considering different load

Fig. 17 The VSI curve (per unit) at **a** the base case and **b** the case with mCapSA optimizer of 33-bus PDG at 24 (h)
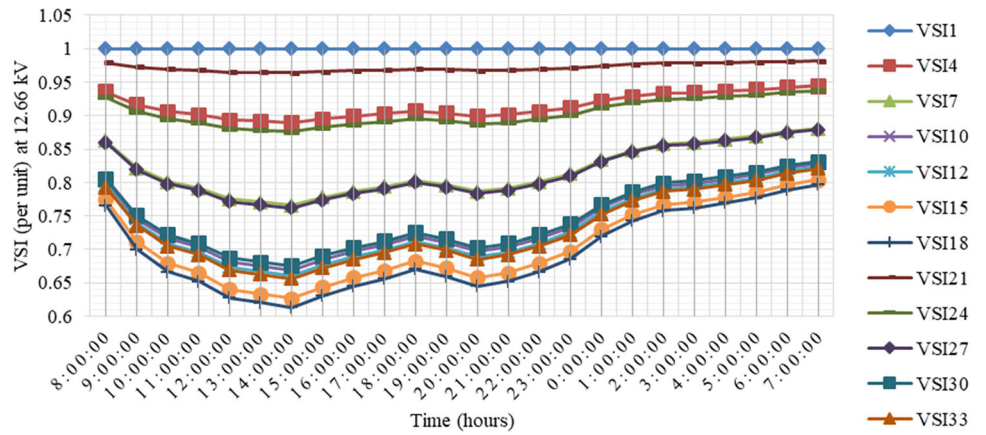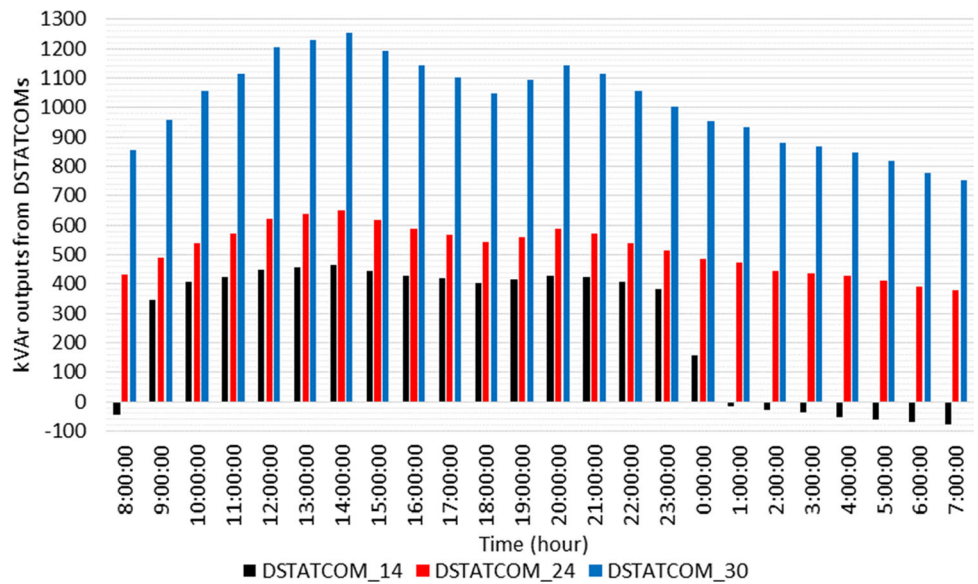

(a)
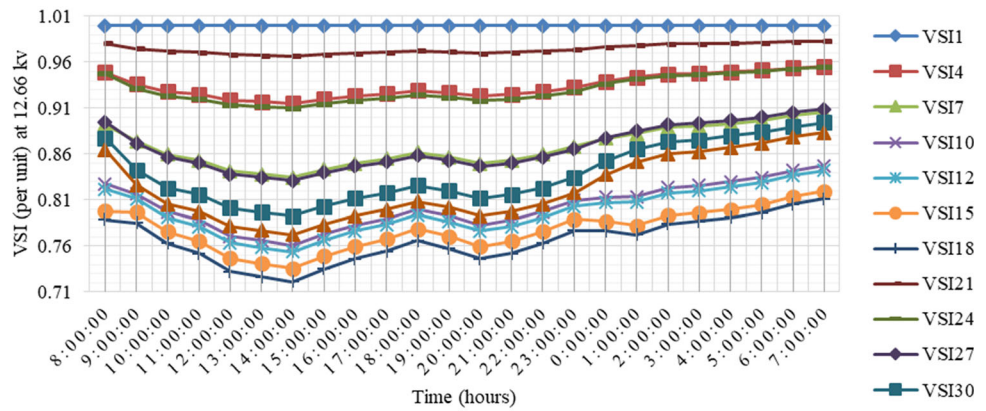
(b)
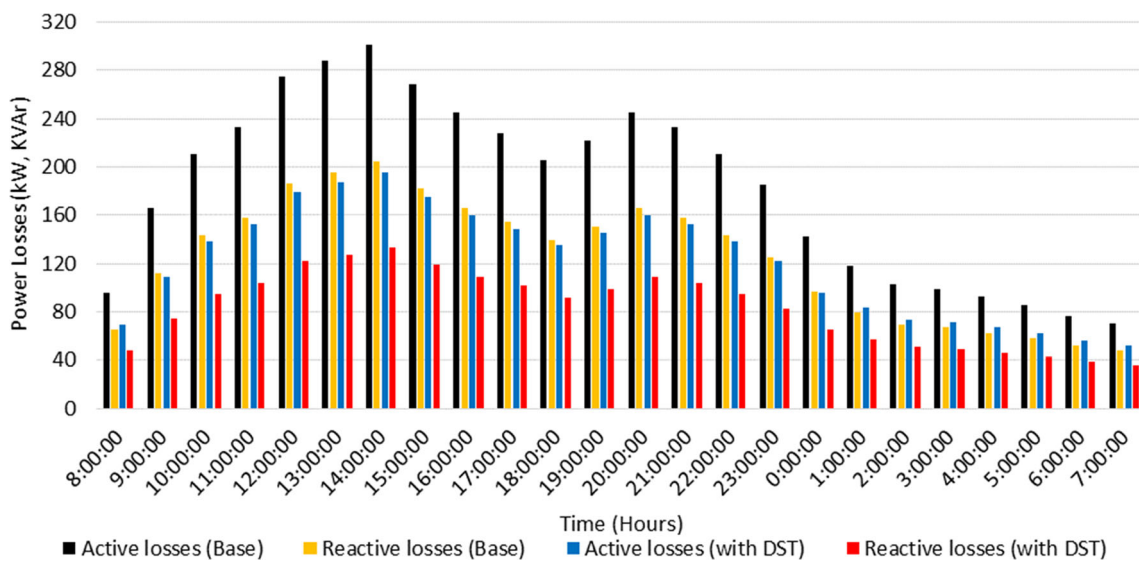
Fig. 18 Hourly kVAr outputs from DSTATCOMs

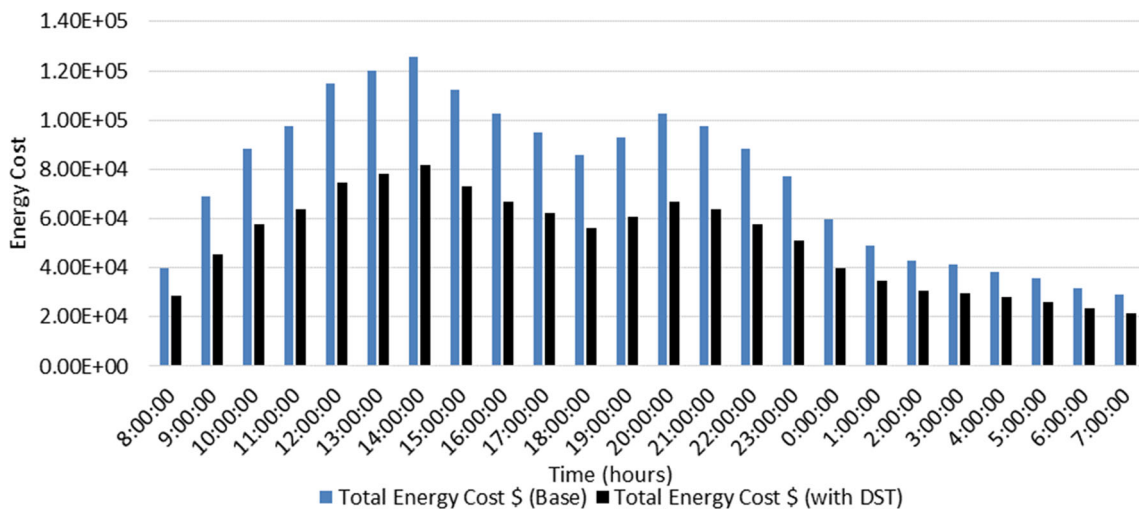**Fig. 19** The total active and reactive power with and without DSTATCOM installations

Fig. 20 The total energy cost with and without DSTATCOM installations
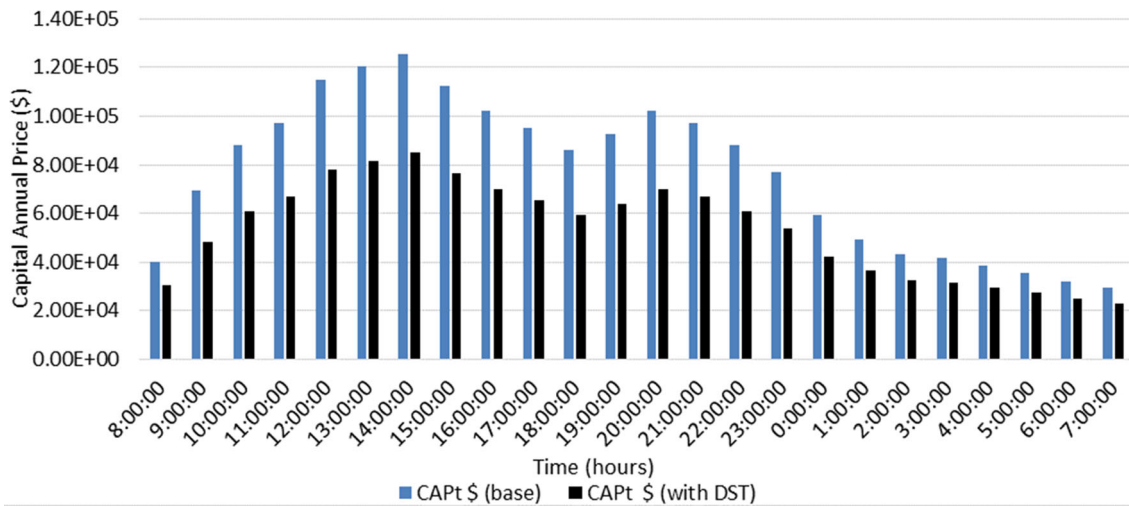
Fig. 21 The capital annual price (CAP_t) with and without DSTATCOM installations

Table 11 The total results of base-case and with DSTATCOM Installations at 24 h (different load conditions)

Items	Base case	DSTATCOM installation
Total active losses (kW)	4398.6637	2926.5481
Active loss reduction (%)	–	33.4673
Total reactive losses (kVAr)	2981.774	2000.489
Reactive loss reduction (%)	–	32.9098
Total energy cost ($)	1,837,649.05	1,222,636.99
Net saving of energy cost ($)	–	615,012.06
Saving of energy cost (%)	–	33.4673
Total purchased price of DSTATCOM ($)	–	61,560.57
Capital annual price ($)	1,837,649.05	1,284,197.56
Net saving of Capital annual price ($)	–	553,451.49
Total saving (%)	–	30.1173

levels using DSTATCOM with distributed generators incorporating distributed storage batteries.

Declaration

Conflict of interest The authors declare that there is no conflict of interest. They have no known competing financial interests or personal relationships that could have appeared to influence the work reported in this paper.

References

1. Ali MH, Mehanna M, Othman E (2020) Optimal planning of RDGs in electrical distribution networks using hybrid SAPSO algorithm. Int J Electr Comput Eng 10:6153. https://doi.org/10.11591/ijece.v10i6.pp6153-6163

2. Tolba MA, Rezk H, Al-Dhaifallah M, Eisa AA (2020) Heuristic optimization techniques for connecting renewable distributed generators on distribution grids. Neural Comput Appl 32:14195–14225. https://doi.org/10.1007/s00521-020-04812-y

3. Rohouma W, Balog RS, Peerzada AA, Begovic MM (2020) D-STATCOM for harmonic mitigation in low voltage distribution network with high penetration of nonlinear loads. Renew Energy 145:1449–1464. https://doi.org/10.1016/j.renene.2019.05.134

4. International Atomic Energy Agency (2017) Industrial applications of nuclear energy. IAEA Nuclear Energy Series No. NP-T-4.3. IAEA, Vienna

5. Tolba MA, Zaki Diab AA, Tulsky VN, Abdelaziz AY (2019) VLCI approach for optimal capacitors allocation in distribution networks based on hybrid PSOGSA optimization algorithm. Neural Comput Appl. https://doi.org/10.1007/s00521-017-3327-7

6. Tolba MA, Tulsky VN, Vanin AS, Diab AAZ (2017) Comprehensive analysis of optimal allocation of capacitor banks in various distribution networks using different hybrid optimization algorithms. In: Conference proceedings—2017 17th IEEE international conference on environment and electrical engineering and 2017 1st IEEE industrial and commercial power systems europe, EEEIC/I and CPS Europe 2017

7. Ahmad AL, A, Sirjani R, (2020) Optimal placement and sizing of multi-type FACTS devices in power systems using metaheuristic optimisation techniques: An updated review. Ain Shams Eng J 11:611–628. https://doi.org/10.1016/j.asej.2019.10.013

8. Hemeida MG, Rezk H, Hamada MM (2018) A comprehensive comparison of STATCOM versus SVC-based fuzzy controller for stability improvement of wind farm connected to multi-machine power system. Electr Eng 100:935–951. https://doi.org/10.1007/s00202-017-0559-6

9. Divan DM, Brumsickle WE, Schneider RS et al (2007) A distributed static series compensator system for realizing active power flow control on existing power lines. IEEE Trans Power Deliv 22:642–649. https://doi.org/10.1109/TPWRD.2006.887103

10. Ali MS, Haque MM, Wolfs P (2019) A review of topological ordering based voltage rise mitigation methods for LV distribution networks with high levels of photovoltaic penetration. Renew Sustain Energy Rev 103:463–476. https://doi.org/10.1016/j.rser.2018.12.049

11. Shehata AA, Tolba MA, El-Rifaie AM, Korovkin NV (2022) Power system operation enhancement using a new hybrid methodology for optimal allocation of FACTS devices. Energy Rep. https://doi.org/10.1016/j.egyr.2021.11.241

12. Bayat A, Bagheri A (2019) Optimal active and reactive power allocation in distribution networks using a novel heuristic approach. Appl Energy 233–234:71–85. https://doi.org/10.1016/j.apenergy.2018.10.030

13. Kazmi SAA, Ameer Khan U, Ahmad HW et al (2020) A techno-economic centric integrated decision-making planning approach for optimal assets placement in meshed distribution network across the load growth. Energies 13:1444. https://doi.org/10.3390/en13061444

14. Kumar C, Mishra MK (2012) A control algorithm for flexible operation of DSTATCOM for power quality improvement in voltage and current control mode. In: 2012 IEEE international conference on power electronics, drives and energy systems (PEDES). IEEE, pp 1–6

15. Wasiak I, Mienski R, Pawelek R, Gburczyk P (2007) Application of DSTATCOM compensators for mitigation of power quality disturbances in low voltage grid with distributed generation. In: 2007 9th international conference on electrical power quality and utilisation. IEEE, pp 1–6

16. Gandoman FH, Ahmadi A, Sharaf AM et al (2018) Review of FACTS technologies and applications for power quality in smart grids with renewable energy systems. Renew Sustain Energy Rev 82:502–514. https://doi.org/10.1016/j.rser.2017.09.062

17. Gitibin R, Hoseinzadeh F (2015) Comparison of D-SVC and D-STATCOM for performance enhancement of the distribution networks connected WECS including voltage dependent load models. In: 2015 20th conference on electrical power distribution networks conference (EPDC). IEEE, pp 90–100

18. Gupta AR, Kumar A (2016) Energy saving using D-STATCOM placement in radial distribution system under reconfigured network. Energy Procedia 90:124–136. https://doi.org/10.1016/j.egypro.2016.11.177

19. Hussain SMS, Subbaramiah M (2013) An analytical approach for optimal location of DSTATCOM in radial distribution system. In: 2013 international conference on energy efficient technologies for sustainability. IEEE, pp 1365–1369

20. Gupta AR, Kumar A (2018) Optimal placement of D-STATCOM using sensitivity approaches in mesh distribution system with time variant load models under load growth. Ain Shams Eng J 9:783–799. https://doi.org/10.1016/j.asej.2016.05.009

21. Yuvaraj T, Ravi K, Devabalaji KR (2017) Optimal allocation of DG and DSTATCOM in radial distribution system using cuckoo search optimization algorithm. Model Simul Eng. https://doi.org/10.1155/2017/2857926

22. Jain A, Gupta AR, Kumar A (2014) An efficient method for D-STATCOM placement in radial distribution system. In: 2014 IEEE 6th India international conference on power electronics (IICPE). IEEE, pp 1–6

23. Gupta AR, Kumar A (2015) Energy savings using D-STATCOM placement in radial distribution system. Procedia Comput Sci 70:558–564. https://doi.org/10.1016/j.procs.2015.10.100

24. Sannigrahi S, Roy Ghatak S, Acharjee P (2019) Strategically incorporation of RES and DSTATCOM for techno-economic-environmental benefits using search space reduction-based ICSA. IET Gener Transm Distrib 13:1369–1381. https://doi.org/10.1049/iet-gtd.2018.5220

25. Shahryari E, Shayeghi H, Moradzadeh M (2018) Probabilistic and multi-objective placement of D-STATCOM in distribution systems considering load uncertainty. Electr Power Compon Syst 46:27–42. https://doi.org/10.1080/15325008.2018.1431819

26. Weqar B, Khan MT, Siddiqui AS (2018) Optimal placement of distributed generation and D-STATCOM in radial distribution network. Smart Sci 6:125–133. https://doi.org/10.1080/23080477.2017.1405625

27. Devi S, Geethanjali M (2014) Optimal location and sizing determination of distributed generation and DSTATCOM using particle swarm optimization algorithm. Int J Electr Power Energy Syst 62:562–570. https://doi.org/10.1016/j.ijepes.2014.05.015

28. Devabalaji KR, Ravi K (2016) Optimal size and siting of multiple DG and DSTATCOM in radial distribution system using Bacterial Foraging Optimization Algorithm. Ain Shams Eng J 7:959–971. https://doi.org/10.1016/j.asej.2015.07.002

29. Khorram-Nia R, Baziar A, Kavousi-Fard A (2013) A novel stochastic framework for the optimal placement and sizing of distribution static compensator. J Intell Learn Syst Appl 05:90–98. https://doi.org/10.4236/jilsa.2013.52010

30. Nazari MH, Khodadadi A, Lorestani A et al (2018) Optimal multi-objective D-STATCOM placement using MOGA for THD mitigation and cost minimization. J Intell Fuzzy Syst 35:2339–2348. https://doi.org/10.3233/JIFS-17698

31. Sanam J, Ganguly S, Panda AK, Hemanth C (2017) Optimization of energy loss cost of distribution networks with the optimal placement and sizing of DSTATCOM using differential evolution algorithm. Arab J Sci Eng 42:2851–2865. https://doi.org/10.1007/s13369-017-2518-y

32. Sannigrahi S, Acharjee P (2018) Implementation of crow search algorithm for optimal allocation of DG and DSTATCOM in practical distribution system. In: 2018 international conference on power, instrumentation, control and computing (PICC). IEEE, pp 1–6

33. Yuvaraj T, Devabalaji KR, Ravi K (2015) Optimal placement and sizing of DSTATCOM using harmony search algorithm. Energy Procedia 79:759–765. https://doi.org/10.1016/j.egypro.2015.11.563

34. Kumar D, Samantaray SR (2016) Implementation of multi-objective seeker-optimization-algorithm for optimal planning of primary distribution systems including DSTATCOM. Int J Electr Power Energy Syst 77:439–449. https://doi.org/10.1016/j.ijepes.2015.11.047

35. Tejaswini V, Susitra D (2020) Dragonfly algorithm for optimal allocation of D-STATCOM in distribution systems, pp 213–228

36. Khan B, Redae K, Gidey E et al (2022) Optimal integration of DSTATCOM using improved bacterial search algorithm for distribution network optimization. Alex Eng J 61:5539–5555. https://doi.org/10.1016/j.aej.2021.11.012

37. Montoya OD, Gil-González W, Hernández JC (2021) Efficient operative cost reduction in distribution grids considering the optimal placement and sizing of D-STATCOMs using a discrete-continuous VSA. Appl Sci 11:2175. https://doi.org/10.3390/app11052175

38. Rezaeian Marjani S, Talavat V, Galvani S (2019) Optimal allocation of D-STATCOM and reconfiguration in radial distribution network using MOPSO algorithm in TOPSIS framework. Int Trans Electr Energy Syst 29:e2723. https://doi.org/10.1002/etep.2723

39. Amin A, Kamel S, Selim A, Nasrat L (2019) Optimal placement of distribution static compensators in radial distribution systems using hybrid analytical-coyote optimization technique. In: 2019 21st international middle east power systems conference (MEPCON). IEEE, pp 982–987

40. Yuvaraj T, Ravi K, Devabalaji KR (2017) DSTATCOM allocation in distribution networks considering load variations using bat algorithm. Ain Shams Eng J 8:391–403. https://doi.org/10.1016/j.asej.2015.08.006

41. Taher SA, Afsari SA (2014) Optimal location and sizing of DSTATCOM in distribution systems by immune algorithm. Int J Electr Power Energy Syst 60:34–44. https://doi.org/10.1016/j.ijepes.2014.02.020

42. Noori A, Zhang Y, Nouri N, Hajivand M (2020) Hybrid allocation of capacitor and distributed static compensator in radial distribution networks using multi-objective improved golden ratio optimization based on fuzzy decision making. IEEE Access 8:162180–162195. https://doi.org/10.1109/ACCESS.2020.2993693

43. Roy Ghatak S, Sannigrahi S, Acharjee P (2018) Comparative performance analysis of DG and DSTATCOM using improved PSO based on success rate for deregulated environment. IEEE Syst J 12:2791–2802. https://doi.org/10.1109/JSYST.2017.2691759

44. Oda ES, El HAMA, Ali A et al (2021) Stochastic optimal planning of distribution system considering integrated photovoltaic-based dg and dstatcom under uncertainties of loads and solar irradiance. IEEE Access 9:26541–26555. https://doi.org/10.1109/ACCESS.2021.3058589

45. Zellagui M, Lasmari A, Settoul S et al (2021) Simultaneous allocation of photovoltaic DG and DSTATCOM for techno-economic and environmental benefits in electrical distribution systems at different loading conditions using novel hybrid optimization algorithms. Int Trans Electr Energy Syst 31:1–35. https://doi.org/10.1002/2050-7038.12992

46. Wolpert DH, Macready WG (1997) No free lunch theorems for optimization. IEEE Trans Evol Comput 1:67–82. https://doi.org/10.1109/4235.585893

47. Braik M, Sheta A, Al-Hiary H (2021) A novel meta-heuristic search algorithm for solving optimization problems: capuchin search algorithm. Neural Comput Appl 33:2515–2547. https://doi.org/10.1007/s00521-020-05145-6

48. Kennedy J, Eberhart R (1995) Particle swarm optimization. In: Proceedings of ICNN'95—international conference on neural networks. IEEE, pp 1942–1948

49. Hansen N, Müller SD, Koumoutsakos P (2003) Reducing the time complexity of the derandomized evolution strategy with covariance matrix adaptation (CMA-ES). Evol Comput 11:1–18. https://doi.org/10.1162/106365603321828970

50. Rashedi E, Nezamabadi-pour H, Saryazdi S (2009) GSA: a gravitational search algorithm. Inf Sci (Ny) 179:2232–2248. https://doi.org/10.1016/j.ins.2009.03.004

51. Mirjalili S, Lewis A (2016) The whale optimization algorithm. Adv Eng Softw 95:51–67. https://doi.org/10.1016/j.advengsoft.2016.01.008

52. Heidari AA, Mirjalili S, Faris H et al (2019) Harris hawks optimization: algorithm and applications. Futur Gener Comput Syst 97:849–872. https://doi.org/10.1016/j.future.2019.02.028

53. Hashim FA, Hussain K, Houssein EH et al (2021) Archimedes optimization algorithm: a new metaheuristic algorithm for solving optimization problems. Appl Intell 51:1531–1551. https://doi.org/10.1007/s10489-020-01893-z

54. Jin J, Rothrock L, McDermott PL, Barnes M (2010) Using the analytic hierarchy process to examine judgment consistency in a complex multiattribute task. IEEE Trans Syst Man Cybern Part A Syst Humans 40:1105–1115. https://doi.org/10.1109/TSMCA.2010.2045119

55. Liu Z, Wen F, Ledwich G (2011) Optimal siting and sizing of distributed generators in distribution systems considering uncertainties. IEEE Trans Power Deliv 26:2541–2551. https://doi.org/10.1109/TPWRD.2011.2165972

56. Ali MH, Mehanna M, Othman E (2020) Optimal network reconfiguration incorporating with renewable energy sources in radial distribution networks optimal network reconfiguration incorporating with renewable energy sources in radial distribution networks

57. Arcuri A, Fraser G (2013) Parameter tuning or default values? An empirical investigation in search-based software engineering. Empir Softw Eng 18:594–623. https://doi.org/10.1007/s10664-013-9249-9

58. Mohamed AW, Hadi AA, Mohamed AK, Awad NH (2020) Evaluating the performance of adaptive gaining sharing knowledge based algorithm on CEC 2020 benchmark problems. In: 2020 IEEE congress on evolutionary computation (CEC). IEEE, pp 1–8

59. Wilcoxon F (1992) Individual comparisons by ranking methods, pp 196–202

60. Dolatabadi SH, Ghorbanian M, Siano P, Hatziargyriou ND (2021) An enhanced IEEE 33 bus benchmark test system for distribution system studies. IEEE Trans Power Syst 36:2565–2572. https://doi.org/10.1109/TPWRS.2020.3038030

61. Zhang D, Fu Z, Zhang L (2007) An improved TS algorithm for loss-minimum reconfiguration in large-scale distribution systems. Electr Power Syst Res 77:685–694. https://doi.org/10.1016/j.epsr.2006.06.005

Springer